Journal of Water Process Engineering 58 (2024) 104733

Contents lists available at ScienceDirect

Journal of Water Process Engineering

journal homepage: www.elsevier.com/locate/jwpe

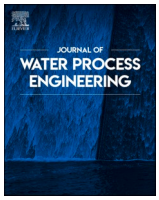

Electro-sorption and -desorption characteristics of electrically conductive polyacrylonitrile membranes to remove aqueous natural organic matter in dead-end ultrafiltration system

Muhammad Usman [a,*], Sarah Glass [b], Tomi Mantel [a], Volkan Filiz [b], Mathias Ernst [a]

[a] Institute of Water Resources and Water Supply, Hamburg University of Technology, Am Schwarzenberg-Campus 3(E), 21073 Hamburg, Germany
[b] Institute of Membrane Research, Helmholtz-Zentrum Hereon, Max-Planck-Straße 1, 21502 Geesthacht, Germany

ARTICLE INFO

Keywords:
Electrical field–assisted UF
NOM characterization
Size exclusion chromatography
Membrane regeneration
DBPs precursors removal
Drinking water treatment

ABSTRACT

Electrically conductive (EC) membranes have emerged as an innovative approach in removing natural organic matter (NOM) by electro-sorption (e-sorption) when external anodic potential (AP) is applied. In this study, the EC membranes were established by a forming a porous nanolayer of Pt nanoparticles via magnetron sputtering on both sides of virgin and chemically modified PAN ultrafiltration (UF) membranes. The modified PAN membranes were functionalized with ethylenediamine (PAN-EDA) and sodium hydroxide (PAN-NaOH). The virgin PAN membrane material contains nitrile group and demonstrated a negative zeta potential in the analyzed pH range. The PAN-EDA membrane owned amidine and amine groups, whereas PAN-NaOH membrane possessed carboxyl and amide groups in the membrane matrix. The PAN-NaOH and PAN-EDA membranes exhibited isoelectric points at 3.7 and 7.8, respectively. Electrical field-assisted UF experiments were conducted with Suwannee River NOM in dead-end mode and NOM removal was monitored using different methods of NOM characterization (e.g., SEC, DOC and UV_{254} absorbance). The results revealed that the non-electrically conductive (NEC) and EC virgin PAN membranes exhibited almost no intrinsic adsorption (at 0 V external potential) and e-sorption of NOM at 2.5 V AP respectively. However, NEC PAN-NaOH and PAN-EDA membranes showed DOC intrinsic sorption loadings of 17 $mg{\cdot}m^{-2}$ and 258 $mg{\cdot}m^{-2}$ at permeate flux 100 $L{\cdot}m^{-2}{\cdot}h^{-1}$ and pH 7 respectively. In comparison, the DOC e-sorption loadings of the EC PAN-NaOH and EC PAN-EDA membranes at 2.5 V AP were 197 $mg{\cdot}m^{-2}$ and 525 $mg{\cdot}m^{-2}$ under same test conditions respectively. The NOM e-desorption characteristics of the EC modified PAN membranes were also investigated to regenerate membranes for a sustainable filtration process. The results indicated that the EC PAN-NaOH and PAN-EDA membranes can be regenerated by reversing the electrical polarity almost completely. In conclusions, the outcomes of this work confirm that the presence of the derivatives of amines (e.g., amines, amidine and amide groups) and carboxyl group are necessary in the membrane matrix to induce e-sorption and -desorption characteristics.

1. Introduction

Natural water resources usually contain variety of organic and inorganic soluble ions/compounds [1,2]. Among organic compounds, humic substances (HSs) having carboxylic acid and phenolic groups in their structure are the prevailing natural organic matter (NOM) in drinking water resources such as surface water and groundwater [3,4]. In addition, HSs can make up to 90 % of the dissolved organic carbon (DOC) [5]. NOM is part of the total organic (TOC), which usually is presented after 0.45 μm filtration as DOC. During the disinfection of drinking water by chlorination, free chlorine may react with fractions of the NOM to create disinfection by-products (DBPs) such as trihalomethanes (THM), haloacetic acids (HAA) and others [1,6,7]. Many DBPs are recognized as detrimental to mankind health [8]. HSs in water typical exhibit higher aromatic carbon content and thus may produce relevant concentrations of DBPs during disinfection [6,7]. Further, the presence of NOM may cause membrane fouling by the irreversible adsorption of organics [9–11], promote undesired bacterial growth in case of no-disinfection [12,13], and impart a yellowish color and/or bad taste/odor [3]. In addition, NOM can bind with heavy metals primarily because of its complexation and possible electrostatic interactions [5].

Membrane separation processes are widely used in drinking water

* Corresponding author.
E-mail address: muhammad.usman@tuhh.de (M. Usman).

https://doi.org/10.1016/j.jwpe.2023.104733
Received 1 September 2023; Received in revised form 30 November 2023; Accepted 22 December 2023
Available online 8 January 2024

treatment especially due to their superior effluent quality, modular flexibility and small physical footprint [14]. To remove NOM, nanofiltration (NF) and/or reverse osmosis (RO) membranes are applied because of high TOC rejection rates (> 90 % of aquatic NOM) [15,16]. However the specific energy consumption (SEC) of those dense membranes is high (up to 4 kWh·m^{-3}) due to high membrane resistance and relatively low molecular weight cut-off characteristic (<100–500 Da) [17,18]. In comparison, ultrafiltration (UF) membranes employed in water treatment mainly for removal of particles including pathogens (e.g., bacteria and viruses) [19–21] are less energy intensive (SEC ≈ 0.3–0.5 kWh·m^{-3} [22]). Conventional UF membranes materials are often polyethersulfone (PES), polyacrylonitrile (PAN) and cellulose acetate (CA) with typical MWCO of 50–200 kDa enable rejection of high molecular weight fractions only [15,23,24]. Consequently, UF can only reject about 10 % of DOC from natural waters. These organics consists of large NOM fractions like biopolymers and low content of HSs [9,15,25].

Various hybrid approaches like coagulation-UF, powdered activated carbon (PAC)-UF or magnetic ion-exchange (MIEX)-UF have been adopted to extend the selectivity of UF membrane processes for DOC as well as to prevent the membrane fouling [9,26–31]. These hybrid UF processes are connected with additional use of chemicals/materials and produce waste streams [9]. Electro-sorption (e-sorption) using porous electrically conductive membranes (ECMs) is an intriguing approach to remove charged molecules (e.g., fractions of NOM) from raw waters [32]. To accomplish these objectives, flow-through electrode configuration is used and the electrical potential difference in the range of 0.5 V to 2.5 V across the electrodes is applied as a driving force [33,34].

The concept of EC membranes (ECMs) has been considered to increase not only the selectivity but also mitigate fouling of membranes by many fold increase in research for both, water and wastewater treatment. The ECMs have been used to induce electrically driven physical and chemical phenomena including electrostatic interactions (significant attractive or repulsive forces, depending on the applied potential, may be induced on charged organics/ions), electrophoresis, electro-osmosis and electro-chemically induced redox reactions like electro-oxidation [14,33–39]. Most of the studies are focused on (organic) fouling mitigation [38,40], selectivity improvement by local pH change [39], removal of NOM and heavy metal ions either by induced repulsive electrostatic force [35,36] or by attractive electrostatic force [32]. It is important to recognize that various researchers have reported the selective e-sorption of ions (e.g., Li^+, NO_3^- Ca^{2+}, Na^+, and Cl^-) and heavy metal ions on porous carbon/polymer composite electrodes for desalination and water purification, as well as for recovery of nutrients (e.g., NH_4^+, and PO_4^{3-}) from wastewater in flow-between (or flow-by) configuration [41–44]. However, there are scanty investigations on e-sorption of dissolved organic water constituents using porous ECM and subsequent regeneration of membrane in a flow-through electrode configuration relevant to dead-end membrane filtration systems [32]. This mode of operation is known for high recoveries in practical applications. The hypothesis coming out of our previous study on NOM e-sorption using dead-end ECMs is that the membrane materials with positive zeta potential might be better suited for the e-sorption/−desorption process [32]. To the best of our knowledge, there is no comprehensive study that has investigated the role of functional groups in the matrix of membrane materials leading to different surface potentials on the membrane surface and thus, e-sorption/−desorption property.

To fill the above-mentioned knowledge gap, the effect of different chemical functional groups, existing in the ECMs matrix, on NOM e-sorption and e-desorption characteristics was studied in an electrical field-assisted dead-end UF system. In this work, we investigated ECM as a working electrode for NOM e-sorption in flow-through configuration to provide a suitable alternative to existing NOM removal techniques (e.g., NF) due to its potentially low energy consumption and selective removal of charged NOM molecules. Moreover, the NOM e-sorption on ECMs in dead-end UF systems for drinking water treatment can be combined with the retention of particles like pathogens (e.g., viruses and bacteria). To establish ECMs, the virgin and two chemically modified PAN membrane materials having different functional groups were used. Virgin modified PAN membranes carried derivatives of amine, nitrile and carboxyl groups as active group. These functional groups led to different surface potentials (negative vs. positive zeta potential) under neutral pH conditions. The ECMs based on virgin PAN, PAN-NaOH and PAN-EDA membranes were established by coating a porous nanolayer of platinum (Pt) nanoparticles (NPs) using magnetron sputtering on both sides (duplex coating) of the membranes. We evaluated the hypothesis by carrying out electrical-field assisted UF experiments if derivatives of amine (amine, amide and amidine groups) are imperative to induce e-sorption characteristics to the membranes under anodic charging. The mechanism of e-sorption process was elucidated using size exclusion chromatography combined with organic carbon detection, DOC analyzes and UV absorbance at 254 nm (UV_{254}). In addition, e-desorption characteristic of ECMs based on modified PAN membranes was investigated under cathodic charging with the aim to optimize the membrane regeneration process without chemicals. Finally, the cyclic operation of ECMs for e-sorption and e-desorption was exercised with aim of developing an application-oriented UF system for continuous NOM removal and membrane regeneration that can be applied for extended filtration time with negligible membrane fouling.

2. Material and methods

2.1. Feed solution

The NOM standard used for the experiments was Suwanee River NOM (SRNOM, 2R101N) procured by the International Humic Substances Society (IHSS, Denver, CO, USA). Benecke, [15] examined the NOM removal rates of SRNOM for 150 kD PES UF membranes and found a maximum DOC rejection of 2 %. Accordingly, we considered this NOM standard ideal for investigations on e-sorption and e-desorption with EC UF membranes. To understand the removal of SRNOM via e-sorption on ECMs, the information on the total acidity of the NOM/HSs is vital. Total acidity is the sum of acidity due to carboxyl and phenolic groups. For SRNOM, the total acidity is 7.3 meq·C^{-1}, which is lower than the acidity of a standard fulvic acid solution tested (8 meq·C^{-1}) [45]. A higher total acidity represents a larger proportion of negatively charged functional groups than a lower total acidity.

The stock solution of concentration 300 mg SRNOM·L^{-1} was prepared by dissolving the sample in deionized (DI) water and shaking it at 150 rpm for one week. After preparation, the stock solution was passed through 0.45 μm cellulose acetate (CA) filter to separate suspended particles from the solution. It was later added to establish 12 mg SRNOM·L^{-1} feedwater concentration (≈ 5 mg DOC L^{-1}) using DI water. The specific ultraviolet absorbance (SUVA) value, an indicator of aromaticity, of the feed water, was 3.9 L·mg^{-1}·m^{-1}. The ionic strength of the feed was adjusted to 1 mmol/L by dosing NaCl and pH was set to pH 7 by titration of 0.1 M NaOH. NaCl and NaOH were procured from Carl Roth GmbH + Co KG, Germany. A portable analytical multimeter Multi 3620 IDS from WTW Xylem GmbH, Weilheim Germany, was used to regulate the pH and electrical conductivity of the feed solution.

2.2. Virgin and modified PAN UF membranes

The virgin polyacrylonitrile (PAN) UF membranes were modified with ethylenediamine (EDA) or NaOH, respectively, as base materials for the formation of ECMs. The PAN membranes having a size of 5 cm × 10 cm were functionalized by EDA as described before [46,47]. The modification of PAN with NaOH was discussed elsewhere [48]. The virgin and modified PAN membranes were composed of a non-woven polyphenylene sulfide (PPS) support layer to provide mechanical integrity to the thin active layer. In the previous studies, we provide characterization of the unmodified, modified PAN membranes using attenuated total reflection Fourier-transform infrared spectroscopy

(ATR-FTIR). The unmodified PAN membrane carried nitrile group as active functional group in the membrane matrix. The PAN-EDA membrane owned amidine and amine groups, whereas PAN-NaOH membrane possessed carboxyl and amide groups. The pore size of the virgin PAN membrane was 12.6 nm ± 6.7 nm and surface porosity was 11.7 ± 1.3 %. In comparison, the average pore sizes of the PAN-NaOH and PAN-EDA membranes were 11.9 nm ± 6.2 nm and 12.2 nm ± 6.1 nm respectively. The average surface porosities of the PAN-NaOH and PAN-EDA were 6.9 % ± 1.2 % and 9.3 % ± 0.6 % [48].

2.3. Establishment of EC PAN-based membranes

For the formation of ECMs, a sputter deposition technique was applied using Sputter Coater SCD 005 (Baltec Inc., Balzers, Lichtenstein), which is a bench scale sputtering device capable of producing nanothin nanolayers of various metals by DC magnetron sputtering. To establish EC PAN-based membranes in this study, three metals such as Au, Pt, and silver (Ag) were investigated in preliminary NOM e-sorption experiments. These investigations showed corrosion of Ag in chloride-rich environments. The corrosion mechanism usually starts with the reaction of Ag with Cl^- ions, leading to the formation of AgCl on the membrane surface. This is followed by the detachment of AgCl into the solution, leading to electrical disconnect of the Ag coating [49]. Au NPs forming nanolayer on the membrane working electrode lost stability in long term e-sorption experiments. Au coated membranes were unable to effectively conduct and distribute the external applied electrical potentials (either anodic or cathodic) across the whole membrane surface, resulting in a sharp decrease in current density. In comparison, EC PAN membranes based on a nanolayer coating (20 nm) of Pt NPs have shown stable porous Pt layer. Hence, Pt was used to implement electrical conductivity at the membrane surface. The thickness of Pt nanolayer was optimized in preliminary NOM e-sorption experiments. Pt nanolayers with 10 nm and 20 nm thickness were investigated. The obtained membrane exhibited an electrical conductivity of 1.62×10^5 S/m and 2.42×10^5 S/m for 10 and 20 nm Pt nanolayers, respectively. With a 10 nm Pt nanolayer, the PAN-EDA membrane was not fully coated as reflected by the SEM image (Fig. 1 SI). As a result, the electrical conductivity was lower for 10 nm Pt sputtered PAN-EDA membrane. When comparing the e-sorption rates of 10 nm and 20 nm Pt sputtered PAN-EDA membranes, PAN-EDA with 10 nm nanolayers yielded lower NOM e-sorption rates, as detected with UV at 254 nm (UV_{254}) in the initial phase of the NOM breakthrough curves (Fig. 2 SI). Further investigations were carried out with 20 nm Pt nanolayers on both sides of the virgin and modified PAN UF membranes for the filtration experiments. Henceforth, the membranes without and with Pt coating were referred to as non-electrically conductive (NEC) and electrically conductive (EC) membranes.

2.3.1. Characterization of virgin and modified PAN membranes

2.3.1.1. Pure water permeability. The measurement of pure water permeability (PWP) provides information about the pore size and the number of pores on the membrane. A higher PWP reflects that there are either low numbers of larger pores or higher numbers of smaller pores. Hence, the PWP of the uncoated and conductive membranes were measured in dead-end mode at the beginning of all electrical field-assisted UF filtration tests. Before the experiments, around 500 mL of DI water was passed through each membrane at 0.5 bar and room temperature (22 ± 2 °C) to determine the PWP and evaluate reproducibility of PWP. Flow rates were measured using the Cori-flow meter (M14-AGD-22-0-S, Bronkhorst Deutschland Nord GmbH, Kamen, Germany). Finally, the PWP was calculated using the following expression:

$$\mathrm{PWP} = \frac{Q}{A_m \cdot \mathrm{TMP}} \quad (1)$$

where Q is the flow rate in $L \cdot h^{-1}$, A_m is the active membrane area in m^2 and TMP is the transmembrane pressure in bar. The PWP was measured in unit of $L \cdot m^{-2} \cdot h^{-1} \cdot bar^{-1}$.

2.3.1.2. Water contact angle. The water contact angle (WCA) of NEC and EC membranes was measured to assess the membrane hydrophilicity before and after coating with Pt using the sessile drop method. The active layer of the membrane was placed exposed to the environment, and 1 mL syringe was used to place droplets of DI water on its surface. Both left and right contact angles were measured, More information on measurement of WCA can be accessed in our former study [50].

2.3.1.3. Zeta potential. The zeta potential of the membranes was calculated using Surpass equipment provided by Anton Paar GmbH, Graz, Austria. The zeta potential was determined by the streaming potential method. The ionic strength and pH were adjusted using KCl and KOH respectively. During the measurement, the streaming solution is titrated against HCl from pH 9 to 3. Further details on zeta potential measurement are documented in Luxbacher, [51]. Each measurement was repeated twice.

2.3.1.4. Scanning electron microscopy. The scanning electron microscopy (SEM) images were recorded on a Merlin SEM (Zeiss, Jena, Germany) at an accelerating voltage of 3 keV using an InLens secondary electron detector. Additional details on SEM are provided in Kishore Chand et al. [48].

2.4. Electrical field-assisted membrane filtration setup

The experimental setup consists of a CF042 flat sheet membrane cell manufactured by Sterlich, Kent, WA (USA), with an active membrane surface of 42 cm^2 (Fig. 1). After placing the membrane, the cell was assembled using nut and bolt connections on four corners. The electrical connections to the membrane were provided by means of thin strips of titanium foils, which in turn were connected to the potentiostat (IPS Elektroniklabor GmbH, Münster, Germany).

For pumping the feed solution, a magnetic coupled gear pump (Bronkhorst Deutschland Nord GmbH, Kamen, Germany) was used. The outlet of the membrane was attached to Spectrophotometer (DR6000, Hach Lange GmbH, Düsseldorf, Germany) for analysis of ultraviolet absorbance at 254 nm (UV_{254}) using 1 in. flow-through cuvette supplied with the photometer and ultimately, leading to the permeate tank. The pressure at the inlet and out of the membrane filtration cell was recorded by pressure sensors (Bronkhorst Deutschland Nord GmbH, Kamen, Germany) every 5 s. Permeate and desorbate were collected in separate containers for NOM characterization. In all experiments, fresh NEC and EC membranes were used for all filtration tests.

The electrical field-assisted filtration experiments were conducted with cell potentials of 1.5, 2.0 and 2.5 V at a constant permeate flux of 100 $L \cdot m^{-2} \cdot h^{-1}$. Anodic potential (AP) of >2.5 V on membrane working electrode was not chosen to avoid water splitting. When the cell potential is higher than the decomposition potential of water, the generation of electro-generated oxidants can occur heterogeneously from water splitting at the surface of anode [33]. The cyclic voltammogram of Pt showed that water splitting will observe at potential >1.2 V vs. Ag/AgCl (Fig. 3 SI). The cell potential equivalent to 1.2 V vs. Ag/AgCl is 2.5 V (Fig. 4 SI).

In all filtration tests, the cell potential was held constant and the current was measured with a potentiostat. The active side (feed side) of the ECM was functioning as the working electrode, whereas the support side as the counter electrode. Anodic (positive) and cathodic (negative) cell potentials were applied to the membrane working electrode during e-sorption and e-desorption cycles, respectively. Similarly, cathodic potential (CP) and anodic potential (AP) was imposed to the membrane counter electrode. Such a configuration of membrane electrodes

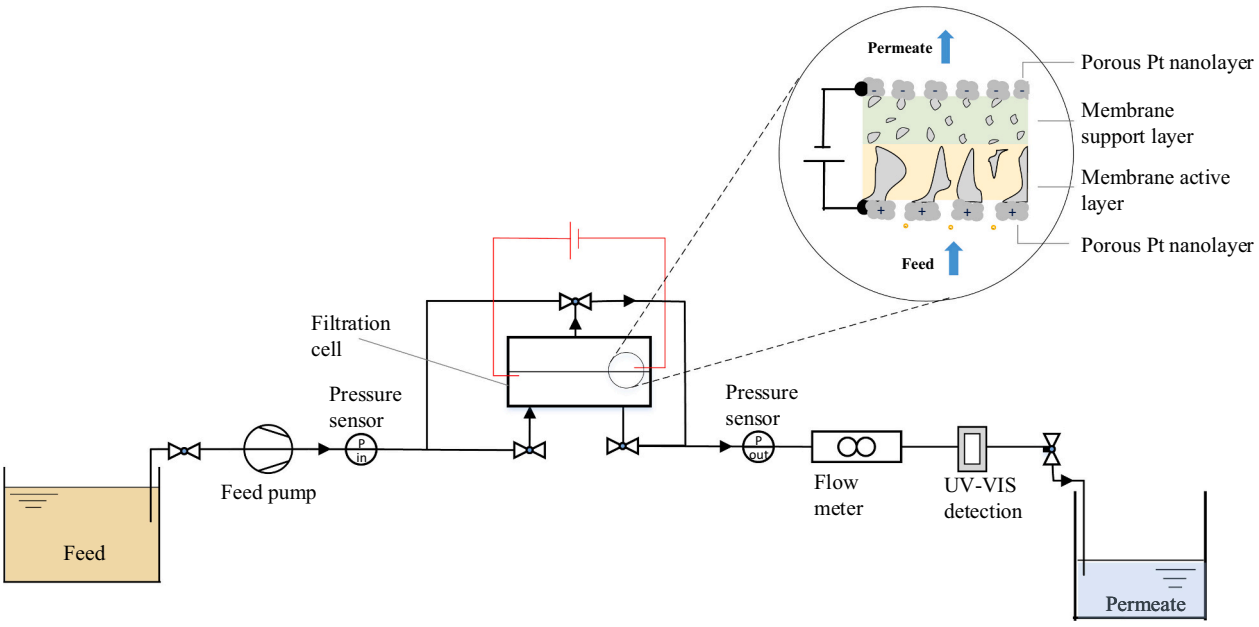

Fig. 1. Schematic representation of the fully automatic dead-end electrical field-assisted UF unit. Inset demonstrates the orientation of the ECM in a membrane filtration cell. The thicknesses of the various layers are not scaled.

excludes the necessity of the additional counter-electrode in the membrane module and thus, makes the design of flat sheet modules more simple [32].

2.5. NOM characterization

The DOC in the feed and permeate samples was measured using a total organic carbon analysis (TOC, Shimadzu, Kyoto, Japan) analyzer. In addition to DOC, organics in feed and permeate samples were characterized by liquid chromatography-organic carbon detection (LC-OCD, DOC-Labor GmbH, Karlsruhe, Germany). LC-OCD is a size–exclusion chromatographic (SEC) procedure combined with both ultraviolet (UV) and organic carbon (OC) detection facility. The five major fractions measured in this method are: biopolymers (> 20,000 $g \cdot mol^{-1}$), HSs (300–1200 $g \cdot mol^{-1}$), building blocks (breakdown product of HSs) (300–500 $g \cdot mol^{-1}$), low molecular weight (LMW) acids and neutrals (<350 $g \cdot mol^{-1}$) [15,52]. Further information on instrument, analytical method, and data interpretation are presented somewhere else [53]. The SEC column had a fractionation range of 100–10,000 $g \cdot mol^{-1}$. The UV detector provides an online UV signal and OC detection is enabled by an infrared (IR) detector after oxidation of NOM to CO_2 in a Graentzel Thin-Film Reactor. SEC chromatograms were interpreted with customized software (ChromCALC, DOC-Labor GmbH, Karlsruhe, Germany).

3. Results and discussion

3.1. Membrane characterization

The PWP and WCA of all applied membranes are shown in Fig. 2. The PWP of the NEC PAN was 1876 $L \cdot m^2 \cdot h^{-1} \cdot bar^{-1}$. In comparison, the PWP of NEC PAN-EDA and PAN-NaOH membranes was 1770 and 1650 $L \cdot m^2 \cdot h^{-1} \cdot bar^{-1}$. After chemical modification, the maximum reduction in PWP was 12 % for PAN-NaOH, indicating the pore size has been only slightly reduced. These results are consistent with pore size of the all membranes. The virgin PAN has the largest pore size followed by PAN-EDA and PAN-NaOH. After formation of ECMs, the PWP of the all PAN-membranes were reduced. The decrease in case of virgin PAN membrane was 30 %. In case of PAN-EDA and PAN-NaOH membranes, the decrease in PWP was 27 and 28 % respectively.

A WCA < 90° indicates a membrane surface with hydrophilic character. The NEC PAN membrane demonstrated a WCA of 46.4°, whereas NEC PAN-EDA and the PAN-NaOH was 41.6° and 43.5° respectively. A slightly lower WCA of the modified PAN membranes than virgin PAN membrane was attributed to the presence of the hydrophilic groups (e.g., carboxyl group and derivatives of amine) in the membrane matrix [48]. After establishment of ECMs, the hydrophilicity of the EC modified PAN membranes were slightly decreased (WCA increased by 3–4 %). The minor increase in WCA might be explained by decreasing surface porosity, pore diameter and pore size.

distribution of the EC membranes compared to NEC membranes

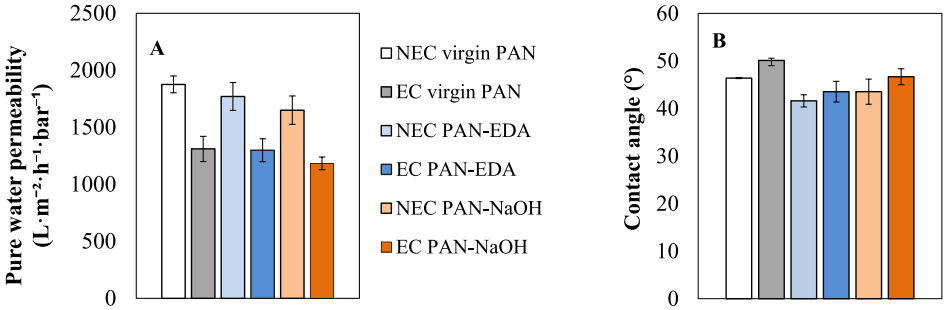

Fig. 2. (A) Pure water permeability, and (B) water contact angle of non-electrically conductive (NEC) and electrically conductive (EC) PAN membranes.

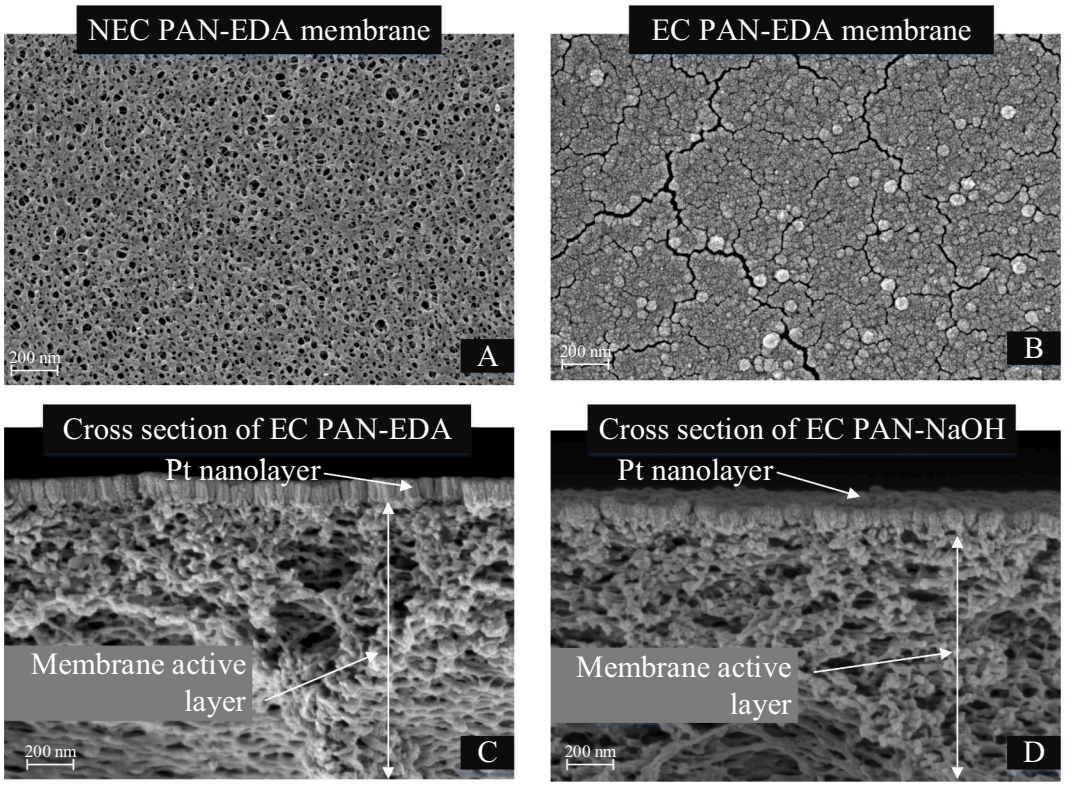

Fig. 3. SEM imaging of (A) NEC PAN-EDA membrane; (B) EC PAN-EDA membrane; (C) cross-section of EC PAN-EDA membrane and (D) EC PAN-NaOH membrane with 50 K magnification.

(Fig. 3). In addition, it has been shown that the surface roughness of metal sputtered membranes increases and pore size distribution decreases due to the deposition of Pt NPs onto the membrane surface, causing a decrease in the membrane porosity [54]. According to Krainer and Hirn [55], the measured WCA increases with decreasing porosity, pore diameter, and water permeability of the membrane material.

The coating of the active and support layer of the membrane with Pt NPs led to significant changes at membrane surface of (Fig. 3). Active and support sides of the ECM are entirely covered with Pt NPs. SEM images of the EC membranes were carried out to study cross-section morphology. The SEM images show a porous nanolayer of Pt and a very porous, sponge-like structure of membrane (Fig. 3C and D). The Pt NPs forming a nanolayer were accumulated only at the membrane surface and the deeper membrane matrix was free of Pt NPs. At the ECM surface, the interconnected cracks appeared in the porous Pt nanolayer (Fig. 3B) and these cracks allowed the water to flow through the Pt sputtered membranes, as evidenced by relatively high water permeability (> 1000 $L \cdot m^2 \cdot h^{-1} \cdot bar^{-1}$ for all ECMs). In addition, small pores can be seen in the porous Pt nanolayer.

It can be observed in Fig. 4 that the zeta potential of virgin PAN membrane was completely negative in the pH range from 9 to 3; isoelectrical point (IEP) was not detectable. Compared to the virgin PAN membrane, the zeta potentials of the modified PAN membranes were increased. The PAN-NaOH membrane showed a zeta potential ranging

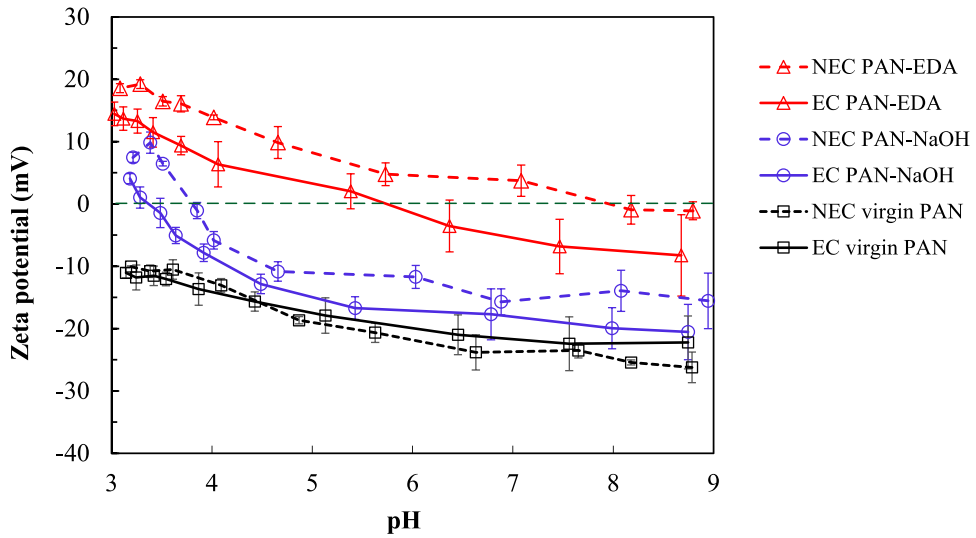

Fig. 4. Zeta potentials of NEC and EC PAN-based UF membranes; streaming potential method in 1 $mmol \cdot L^{-1}$ KCl; error bars present standard deviations ($n = 2$).

from −15 mV to 7 mV with an IEP at pH 3.7. The IEP was recognizable due to the protonation of COO- to COOH. Similarly, the increase in the zeta potential of the PAN-EDA membrane was higher compared to PAN-NaOH membrane probably due to protonation of amine groups ($-NH_2$) in EDA to cationic form ($-NH_3^+$) to higher extent in acidic solution [56] and as a result, IEP of PAN-EDA was at 7.8.

After coating with Pt NPs via magnetron sputtering, the zeta potential of EC PAN-EDA and EC PAN-NaOH was shifted towards lower values. This might be explained by the charge properties of Pt nanoparticles as well as of pure Pt surface, as the zeta potential of Pt nanoparticles is negatively charged over the entire pH range [57–59]. The IEP of EC PAN-EDA and EC PAN-NaOH are 5.8 and 3.2 compared to 7.8 and 3.7 for NEC PAN-EDA and PAN-NaOH membrane, respectively. The effect of Pt NPs forming porous film was negligible because both the Pt NPs and virgin PAN membrane own negative surface charge.

3.2. NOM intrinsic and e-sorption characteristics of virgin and modified PAN UF membranes

To investigate the intrinsic sorption characteristics of the three membrane materials (virgin PAN and modified PAN), breakthrough of NOM, detected using the absorbance at 254 nm (UV_{254}) on NEC membranes without imposing external APs was studied and the results are presented in Fig. 5A. Each experiment was performed until the adsorption equilibrium was reached ($C/C_0 = 1$). Fig. 5A shows NOM, as reflected by relative UV_{254} absorbance, was not removed by NEC virgin PAN membrane in dead-end filtration. The same is true for NEC PAN-NaOH as this exhibit minor intrinsic adsorption only (fully saturated after 5 min). The PAN-NaOH membrane has amide group as functional group in its matrix. In a former study, comparable findings were observed during SRNOM adsorption on a commercial polyamide membrane material [32]. However, the NEC PAN-EDA membrane showed clearly higher intrinsic NOM adsorption behavior (no external potential applied) at the early stage of dead-end filtration (Fig. 5A). However, within the first hour of filtration the NOM adsorption capacity of PAN-EDA membrane was almost saturated and complete breakthrough ($C/C_o = 1$) of UV_{254} was observed in 2 h. The intrinsic adsorption behavior of PAN-EDA towards NOM might be explained by presence of primary amine functional group [60–62]. EDA functionalized adsorbents have been investigated for adsorption of negatively charged dyes and heavy metals (hexavalent chromium, Cr^{VI}). The mechanisms involved in the adsorption process were found to be the electrostatic interactions between oppositely charged target pollutant and adsorptive media as well as chemisorption through ionic interactions [56,61]. The limited intrinsic NOM adsorption performance of the PAN-EDA membrane might be explained by weak electrostatic attraction force, which results from the small difference between the membrane IEP (pH = 7.3) and the feed solution (pH = 7). As a consequence, the number of positively charged sites on the adsorptive media might be rather low [61]. Hence, this material does not favor the sorption of negatively charged organics such as HSs at neutral pH.

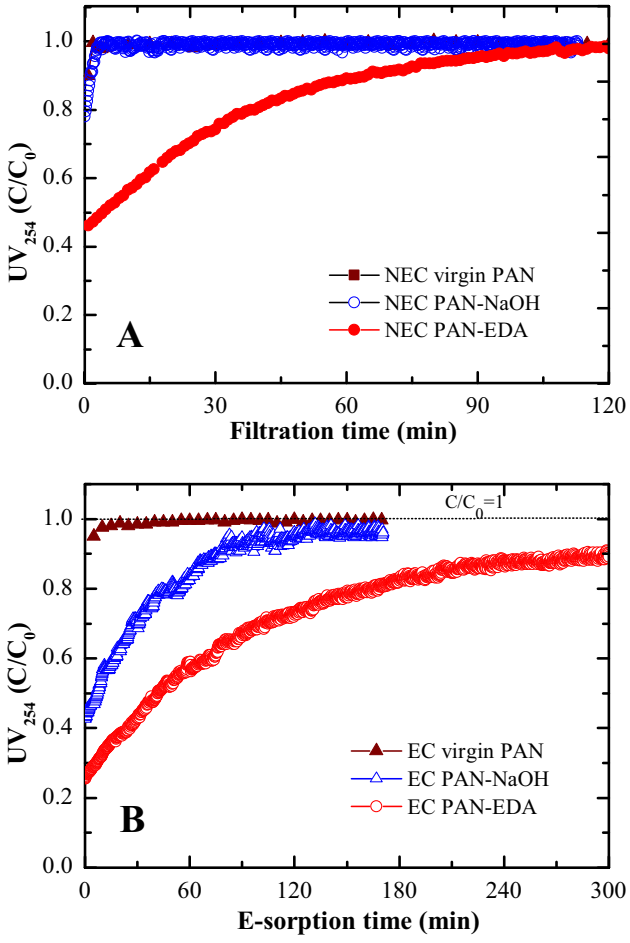

Fig. 5. UV_{254} absorbance curves representing (A) the intrinsic sorption on NEC virgin and modified PAN UF membranes (no external potential applied), and (B) e-sorption on EC virgin and modified PAN UF membranes when AP of 2.5 V was applied at SRNOM= 12 mg·L^{-1}, DOC ≈ 5 mg·L^{-1}, permeate flux = 100 L·m^{-2}·h^{-1}, pH 7 and NaCl = 1 mmol·L^{-1}.

The e-sorption characteristics of the three ECMs were investigated in Fig. 5B. When external AP of 2.5 V was imposed, the EC virgin PAN membrane did not exhibit NOM e-sorption. However, NOM adsorption on EC PAN-NaOH and PAN-EDA membranes was increased significantly compared to NEC PAN-NaOH and PAN-EDA membranes, indicating e-sorption process is responsible for NOM removal. The NOM e-sorption could be mainly attributed to induced electrostatic interactions between negatively charged organic molecules and externally anodically charged ECMs. The presence of amines and its derivatives (e.g., amidine and amide groups) as well as the carboxyl group in the membrane matrix results in better NOM e-sorption properties of the EC modified PAN membranes compared to pristine material. The e-sorption properties of the modified PAN materials might be explained by the polarizability of the functional groups available in the modified membrane matrix. The carboxyl group as well as the amine and its derivatives (e.g., amidine and amide groups) are known for their high polarizability [63]. This applies that the charge of the functional groups is easily shifted when exposed to an electric field [64] and that charge separation is very likely. This charge separation could support NOM e-sorption through the development of electrostatic interactions between charged NOM molecules and the ECM. In comparison, the nitrile group is not easily polarized [63] and therefore is not suitable for the development of ECMs. The increase in NOM sorption, as indicated by UV_{254} removal rates, was large for the EC PAN-EDA membrane. The better NOM performance of EC PAN-EDA could be explained by the combined contributions of intrinsic adsorption and e-sorption property.

The specific DOC surface loadings have been calculated for all experimental setups in Fig. 6. The PAN-NaOH reached 17 mg·m^{-2}, which was increased to 197 mg·m^{-2} by implementing an AP of 2.5 V at ECM surface, indicating an electrostatically enhanced DOC e-sorption of 180 mg·m^{-2}. For the PAN-EDA membrane, the enhanced DOC e-sorption loading was 267 mg·m^{-2}. Higher DOC loads are removed by e-sorption on EC PAN-EDA compared to the EC PAN-NaOH membrane. The lower DOC e-sorption loadings of EC PAN-NaOH membrane compared to EC PAN-EDA might be explained by significantly lower (more negative) zeta potential (~ −15 mV at pH 7) compared to EC PAN-EDA (~ 5 mV at pH 7), which hinders NOM e-sorption when positive external potential is applied to the membrane working electrode.

To illustrate the impact of varying external AP and permeate flux on

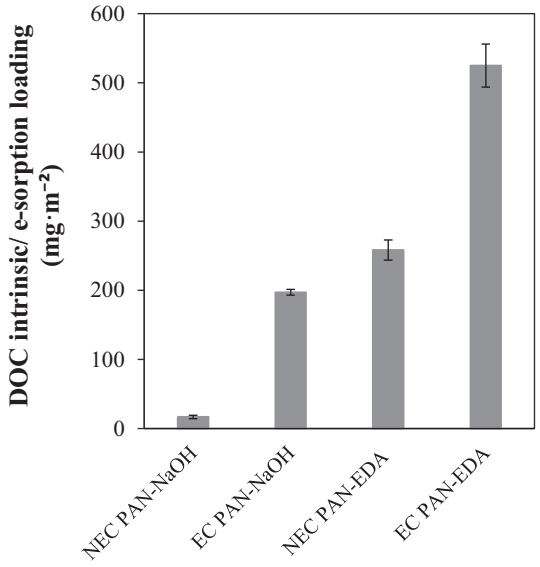

Fig. 6. DOC intrinsic and e-sorption loadings of NEC and EC modified PAN membranes at SRNOM= 12 mg·L^{-1}, DOC ≈ 5 mg·L^{-1}, permeate flux = 100 L·m^{-2}·h^{-1}, NaCl = 1 mmol·L^{-1} and pH 7. The AP of 2.5 V was applied to both ECMs.

NOM e-sorption, further electrical field-assisted UF experiments were carried out using the EC PAN-EDA membrane.

3.2.1. *Impact of external anodic potential and permeate fluxes*

The external applied potential might play a decisive role in driving the charged ions onto the surface of the ECM. In membrane e-sorption technology, the applied voltage influences the electrostatic interactions and pollutant removal efficiency [33,65,66]. For that reason, NOM removal via e-sorption at three APs on the EC PAN-EDA membrane was investigated. The breakthrough curves of UV_{254} and DOC are shown in Fig. 7. The increase in applied voltage exerts high electrostatic force on organic molecules [67] and thereby increases the ion concentration near the ECM surface [36], which could stimulates the ion transport [68] and thus increases the NOM e-sorption capacity, which is reflected by UV_{254} (Fig. 7A). Similar trend can be seen for DOC removal rates (Fig. 7B). Compared to UV_{254}, lower removal rates for DOC were calculated at similar APs. For instance, the UV_{254} removal was 75 %, whereas DOC removal was 52 % at 2.5 V AP (Fig. 7B). Analogous pattern for removal of UV_{254} and DOC was obtained for intrinsic sorption on NEC PAN-EDA membrane. Larger removal of UV_{254} than DOC indicated that e-sorption using EC PAN-EDA membranes and intrinsic sorption using NEC PAN-EDA membranes mainly targeted aromatic moieties contained in the organic molecules. This aromatic NOM fraction in natural waters is usually larger in MW compared to non-aromatic DOC compounds. Higher removal rates for aromatic NOM fractions have been realized for coagulation, dense membrane filtration, for certain activated carbons and ion exchange resins [69–71].

Complete removal of aqueous DOC via e-sorption even at the highest AP of 2.5 V and early stages of sorption was not possible because of the presence of non-responding NOM fractions (e.g., uncharged NOM species). According to the literature, 10–40 % of the NOM cannot be eliminated by ion exchange mechanisms and the presence of uncharged NOM species (e.g., LWM neutrals) is the primary cause of incomplete removal by ion exchange [2,72,73].

The increasing DOC e-sorption loadings show an agreement with increasing APs (Fig. 8A). At the lowest AP of 1.5 V, the DOC e-sorption loading was 356 mg·m^{-2} and at highest AP of 2.5 V, the DOC e-sorption loading was 525 mg·m^{-2}. These results have shown that external AP can influence not only the NOM e-sorption rate, expressed by UV_{254} and DOC removal in Fig. 7 but also DOC e-sorption loadings (Fig. 8A).

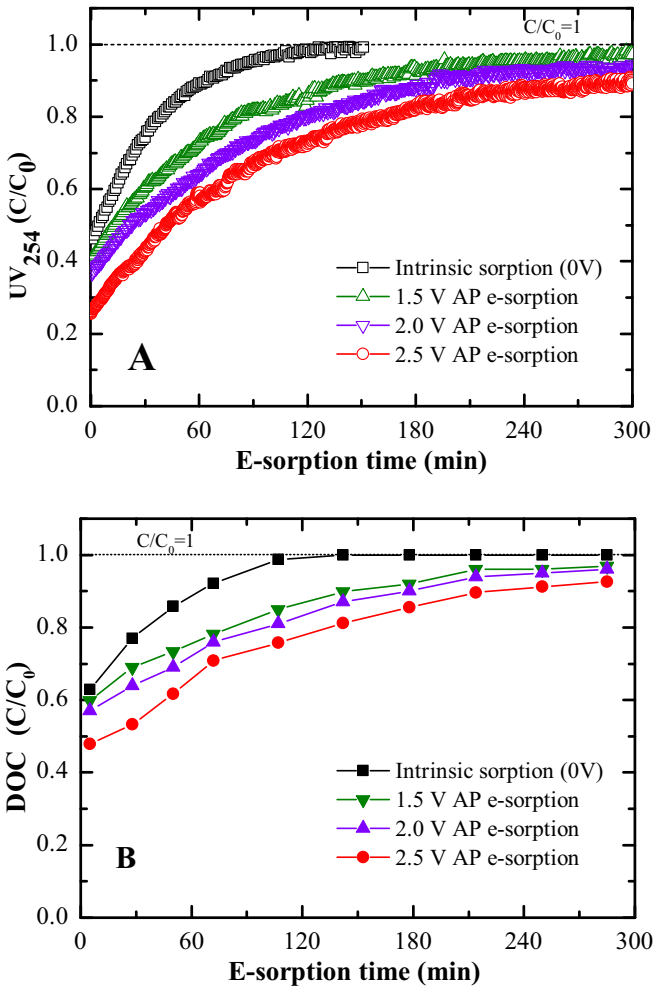

Fig. 7. (A) UV_{254} absorbance curves and (B) DOC breakthrough curves for intrinsic sorption and e-sorption on EC PAN-EDA UF membranes at three different APs at 100 L·m^{-2}·h^{-1} permeate flux. The feed water consisted of DI water with SRNOM = 12 mg·L^{-1}, DOC≈ 5 mg·L^{-1}, NaCl = 1 mmol·L^{-1} at pH 7.

In Fig. 8(B), the effect of permeate flux that reflects the hydraulic retention time (HRT_m) within the membranes' material has been demonstrated. HRT_m was calculated based on membrane thickness (t_m) and permeate velocity (v):

$$HRT_m = \frac{t_m}{v} \quad (2)$$

When AP of 2.5 V was applied, surprisingly a reduced permeate flux had very limited effect on increased DOC e-sorption loadings (Fig. 8B). When the permeate flux was reduced from 100 to 50 L·m^{-2}·h^{-1}, the increase in the DOC e-sorption loading was just 5 %. By further reducing the flux from 100 to 25 L·m^{-2}·h^{-1}, the increase in the DOC e-sorption loading was merely 8 %. The results suggest that increasing the HRT_m from 3.6 to 14 s does not lead to favored DOC removal performance. These results further reflect no change in attribution of electrostatic interactions at a specific external potential at various contact times. Identical trend has been reported during NOM adsorption in GAC filter when the contact time was doubled [74].

3.2.2. *Impact of organics molecular weight on NOM e-sorption efficiency*

In Fig. 9, size exclusion chromatograms obtained with OC and UV detection are compared for feed and permeate samples obtained from intrinsic sorption and e-sorption on NEC and EC PAN-EDA membranes during the first hour of electro-assisted filtration, respectively. The size exclusion chromatogram of the feed that was obtained with OC

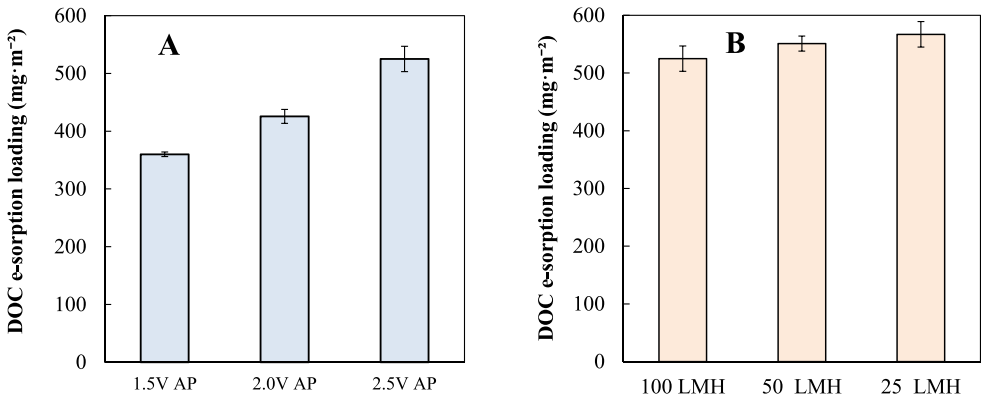

Fig. 8. DOC e-sorption loadings for EC PAN-EDA (A) under varying APs at permeate flux = 100 L·m^{-2}·h^{-1}, and (B) under varying permeate fluxes at 2.5 V AP. SRNOM = 12 mg·L^{-1}, DOC ≈ 5 mg·L^{-1}, pH 7 and NaCl = 1 mmol·L^{-1}.

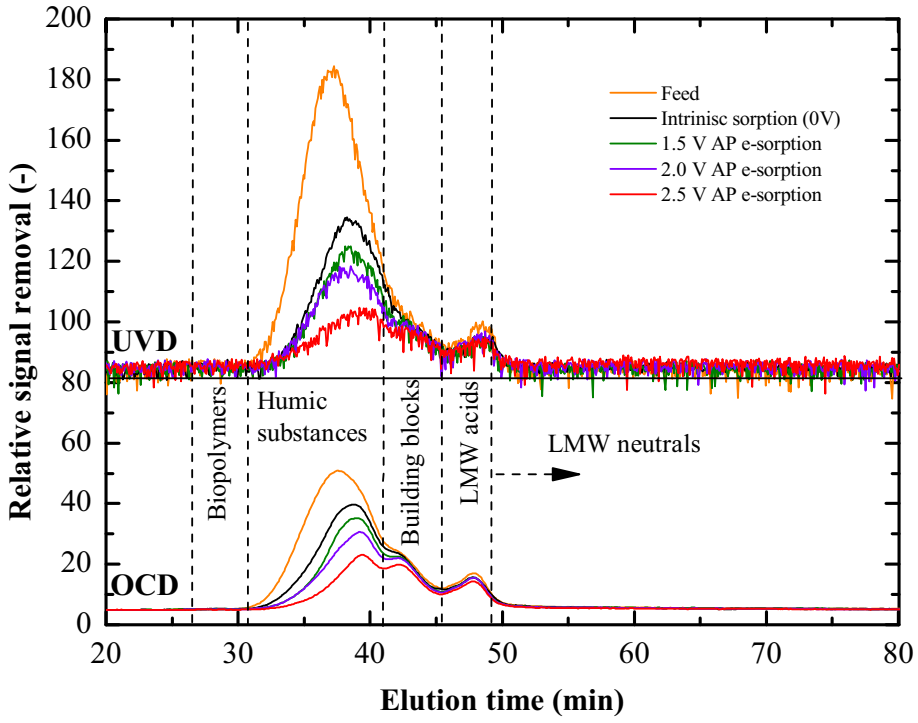

Fig. 9. SEC chromatograms obtained with OCD and UVD for SRNOM feed and permeate samples of one-hour e-sorption at 100 L·m^{-2}·h^{-1} permeate flux. EC PAN-EDA UF membrane was applied under experimental conditions of SRNOM = 12 mg·L^{-1}, DOC ≈ 5 mg/ L, NaCl = 1 mmol·L^{-1} at pH 7.

detection exhibits a peak for HSs (38 min elution time) followed by building blocks (42 elution time) [74]. In some literatures, the term building blocks have been used to indicate HSs-like material of lower MW [53]. LMW acids (48 min elution time) are composed of all aliphatic organics acids that co-elute due to an ion chromatographic effect. LMW humics that elute simultaneously. The LMW neutrals (> 49 min elution time) are neutral or amphiphilic molecules that interact with the SEC column and consequently have a longer elution time [74].

When size exclusion chromatogram obtained with OC detection and with UV detection was compared, UV detection deviates in two aspects: (1) the relative signal removal for HSs compared to other peak is higher, and (2) the relative signal removal for building blocks compared to others is lower. In addition, the peak maxima for biopolymers was absent with both OC and UV detection.

HSs and building blocks were removed through intrinsic adsorption of the material (Fig. 9). With increasing APs, the removal of these NOM fractions increases. Moreover, as the MW of the eluting DOC fractions decreased with the elution time of LC-OCD-UV system [53]. Fig. 9 exhibits that the specific NOM removal rate of compounds with higher MW is higher than for low MW organics. The removal of LMW organics (acids and neutrals) was negligible at 0 V and three APs including the highest AP of 2.5 V. This observation is identical for both chromatograms, either with OC or UV detection.

When higher external cell potentials are applied to the ECMs, electrochemical redox reactions may take place either by oxidation, e. g. through the presence of hydroxyl radical (OH$^{\bullet}$)/reactive oxygen species and/or by electrochemical reduction. The later may be induced by surface adsorbed atomic hydrogen (H*) that can interact with present organics [33,34,36]. However, in Fig. 9, neither new peaks nor larger peaks than peak maxima of the feed sample occurred in the SEC-OCD chromatogram, indicating those electrochemical based redox reactions are not relevant in performed experiments.

The ChromCALC software program allows the calculation of the identified DOC fractions present in all samples and thus, distinguish

between fractions removed by intrinsic NOM sorption as well as by NOM e-sorption (Fig. 10). SRNOM feed contains 5.5 mg/L DOC (LC-OCD bypass measurement) that consists of about 90 % hydrophilic organics. These organics comprised of 79.9 % HSs, 11.9 % building blocks, 4.8 % LMW acids and 3.4 % LMW neutrals.

The intrinsic DOC adsorption results in 23 % removal of hydrophilic HSs and 1 % of building blocks. However, DOC e-sorption at 2.5 V AP was able to eliminate 49 % of hydrophilic HSs, 6 % removal of building blocks and even 2 % removal of LWM acids. These results show that NOM e-sorption by ECMs allows a significant reduction of the HSs concentration, which have been found as precursors for formation of disinfection by-products during chlorination [75,76]. The ECMs energy consumption at AP of 2.5 V (and current density = 2 $A{\cdot}m^{-2}$) was calculated to only 20 $Wh{\cdot}m^{-3}$.

3.2.3. *Impact of porous Pt nanolayer on intrinsic adsorption capacity of EC membranes*

In this work, a porous Pt nanolayer was sputtered on both sides of the UF membranes to establish EC membranes. Thus, the impact of porous Pt nanolayer on intrinsic adsorption capacity of EC membranes was also investigated. Since the NEC PAN-EDA membrane demonstrated intrinsic adsorption for NOM (Fig. 5A). The intrinsic adsorption of NOM on NEC and EC PAN-EDA membranes is shown in Fig. 11.

The EC PAN-EDA membranes exhibits almost identical intrinsic adsorption properties for UV_{254} active compounds compared to the NEC PAN-EDA membrane. The calculated intrinsic adsorption loading of DOC on the EC PAN-EDA membrane was 238 ± 17 $mg{\cdot}m^{-2}$, whereas the DOC intrinsic adsorption loading of the NEC PAN-EDA membrane was 258 ± 10 $mg{\cdot}m^{-2}$ (Fig. 6). Accordingly, the intrinsic DOC adsorption loading of the NEC PAN-EDA membrane was hardly decreased by the coating with Pt NPs. These results reflect that the majority of the adsorption sites are accessible by the NOM molecules in dead-end UF system even after coating with a porous nanolayer of Pt NPs (Fig. 11B) and that the active functional groups on the membrane surface and in the pores are relevant influencing variables. We further conclude that the EC coating by Pt NPs has a negligible impact on intrinsic DOC adsorption capacity of the membrane compared with NEC-PAN

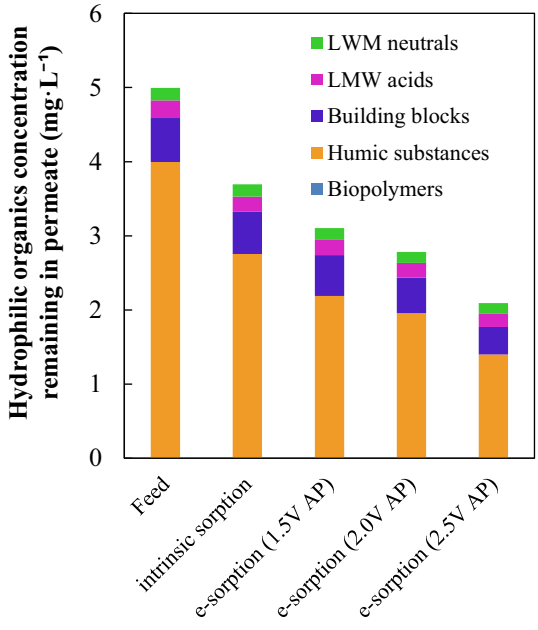

Fig. 10. Concentration of DOC fractions in feed (before experiment) and permeates (after 60 min of e-sorption) for intrinsic adsorption at 0 V and e-sorption at three APs. The EC PAN-EDA UF membrane was investigated for treatment of feed water having SRNOM = 12 $mg{\cdot}L^{-1}$, DOC ≈ 5 $mg{\cdot}L^{-1}$, pH 7 and NaCl = 1 $mmol{\cdot}L^{-1}$ at permeate flux = 100 $L{\cdot}m^{-2}{\cdot}h^{-1}$.

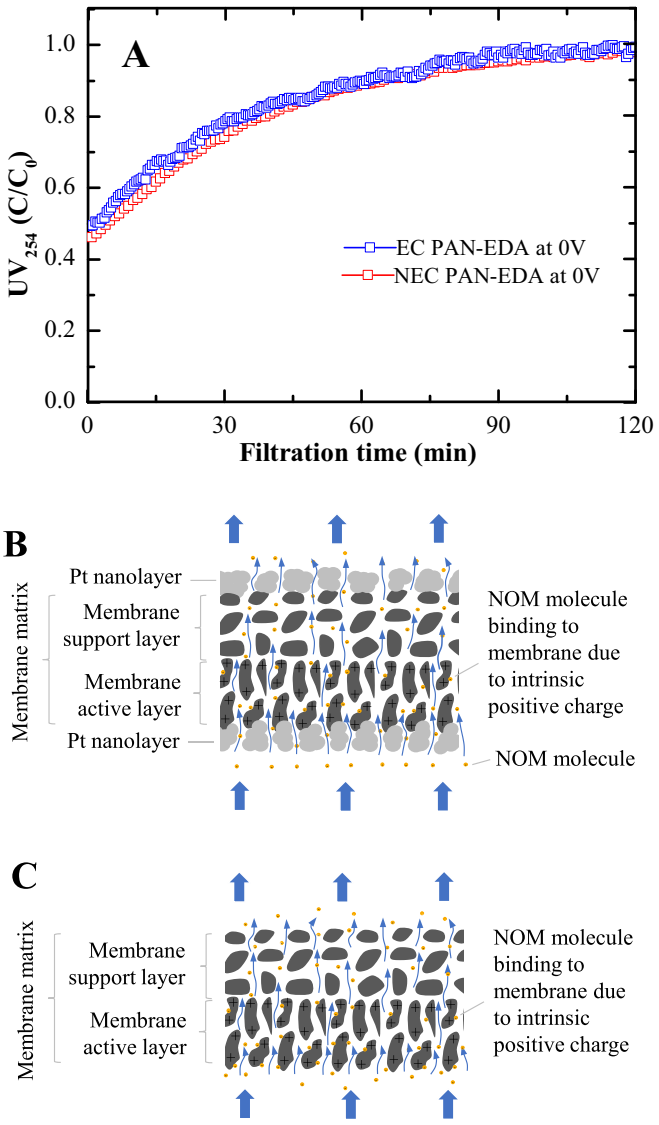

Fig. 11. (A) UV_{254} absorbance curves for intrinsic adsorption of NOM onto NEC and EC PAN-EDA membranes (at 0 V) treating feed water with SRNOM = 12 $mg{\cdot}L^{-1}$, DOC≈ 5 mgL^{-1}, pH 7 and NaCl = 1 $mmol{\cdot}L^{-1}$ at permeate flux = 100 $L{\cdot}m^{-2}{\cdot}h^{-1}$. Schematic representation of convective flow through the pores of (B) EC membrane, and (C) NEC membrane at 0 V (without external potential).

materials. This might be due to the fact that the NPs of coating material form a.

nanolayer at the membrane surface (Fig. 3B and C) and have a slight impact on membrane properties such as water permeability, contact angle, and zeta potential.

3.3. *Characterizing NOM e-desorption on EC modified PAN UF membranes*

The NOM e-sorption removal from Suwannee River on EC PAN-NaOH and PAN-EDA membranes was investigated in dead-end configuration (Fig. 5B). In a large-scale process, the UF filtration will be frequently backwashed to restore permeability (hydrodynamically reversible fouling). During short backwash periods for filter cake removal, it might be feasible to desorb attached NOM via electrostatic repulsion mechanism in an electro-driven membrane process in parallel. Accordingly, in-situ regeneration experiments by NOM e-desorption were executed by reversing the membranes polarity (active site from anodic to cathodic) with the aim to evaluate the potential for sustainable

regeneration of the material. SRNOM solution used as feed water for NOM e-sorption experiments was adopted for NOM/UV_{254} e-desorption experiments. UV_{254} absorbance for EC PAN-EDA and PAN-NaOH ECMs at 2.5 V CP are shown in Fig. 12A. The sharp increase in UV_{254} absorbance, suggests a high release (NOM desorption) of negatively charged organics like HSs from the ECM material by electrostatic repulsion. During the

e-desorption cycle, an electrophoretic force might also occur because the membrane working electrode and adsorbed organics exhibit similar electrical polarity. During NOM e-sorption, it is plausible that a limited amount of NOM fractions smaller than the membrane pore size adsorb to the inner pore surface eventually leading to internal fouling. During e-desorption cycle, the negatively charged NOM fractions are also expected to desorb from inner pore surface due to electrophoretic force and significant repulsive forces between the membrane surface and the charged organic molecules produced by electrostatic interactions, as evidenced by release of large loads of these fractions (Fig. 7 SI).

Fig. 12A further reveals that the NOM e-desorption maxima from EC PAN-EDA was higher ($C/C_o = \approx 3.9$) compared to the EC PAN-NaOH maxima ($C/C_o = \approx 3.2$). For both ECMs, the UV_{254} e-desorption peak appeared between 3 and 5 min (20–35 mL desorbate volume). After the NOM peak, e-desorption is tailing out for both ECMs. This behavior might be explained by decreasing concentration difference between solid-phase organics on and in the ECM surface and liquid-phase organic substances, which decelerates the transport of organic molecules from the ECM surface. An important result is that nearly three-fourth of the

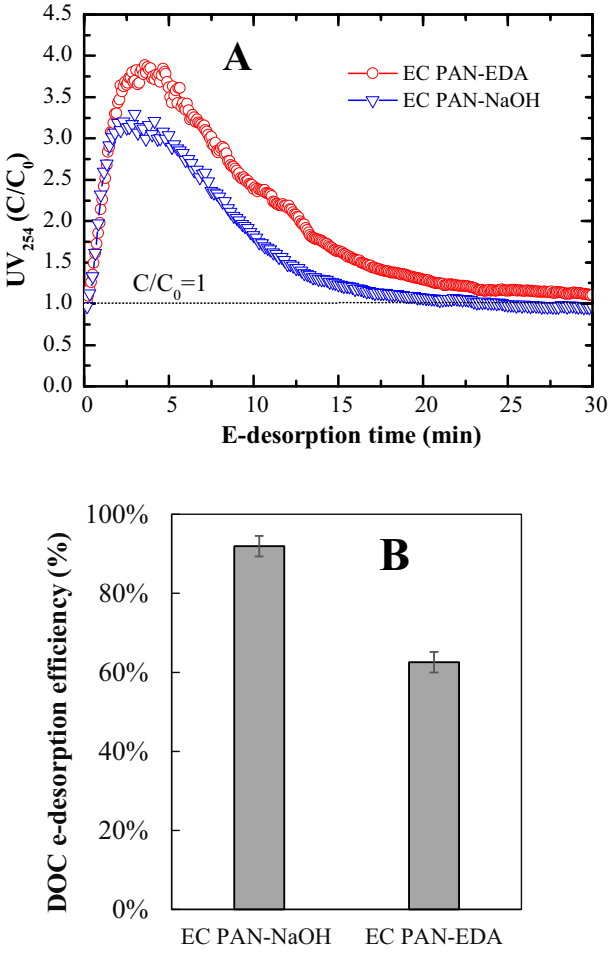

Fig. 12. (A) UV_{254} e-desorption curves, (B) DOC e-desorption efficiency of the EC PAN-EDA and EC PAN-NaOH membranes at cathodic potential = 2.5 V and permeate flux = 100 $L{\cdot}m^{-2}{\cdot}h^{-1}$. The feed water consisted of SRNOM = 12 $mg{\cdot}L^{-1}$, DOC ≈ 5 $mg{\cdot}L^{-1}$, and NaCl = 1 $mmol{\cdot}L^{-1}$ at pH 7.

materials regeneration occurred within first 10 min (70 mL). An ECM demonstrating rapid NOM desorption characteristic would be favorable for large scale application. The e-desorption cycle was completed (when $C/C_o = 1$) earlier on EC PAN-NaOH than EC PAN-EDA mostly likely due to lower DOC accumulation during e-sorption (Fig. 12A).

The NOM e-desorption efficiencies of the both EC modified PAN membranes were calculated (Fig. 12B) using the following Eq. (3):

$$E - desorption\ efficiency = \frac{DOC\ desorbed\ load\ at\ CP}{Total\ DOC\ adsorbed\ load} x\ 100 \quad (3)$$

The DOC adsorbed load takes into account the NOM intrinsic sorption at 0 V and/or e-sorption at AP. The e-desorption efficiency (also referred to as regeneration) of the EC PAN-EDA at 2.5 V CP was 63 %, whereas EC PAN-NAOH membrane was more efficiently regenerated (92 %). In the case of the EC PAN-NAOH membrane, the majority of the NOM (about 91 %) was removed by means of e-sorption and 9 % NOM was removed by intrinsic sorption (Figs. 5 and 6). During e-desorption cycle, all of the organic substances adsorbed by e-sorption might have electrically desorbed from the ECM surface, which leads to very high NOM e-desorption efficiency of the EC PAN-NaOH. In the case of the EC PAN-EDA membrane, the contribution of external NOM e-sorption was about 50 % (Figs. 5 and 6). It might be possible that the NOM adsorption by means of intrinsic sorption was irreversible for e-desorption and contributed to incomplete regeneration of the EC PAN-EDA membrane. To explain incomplete regeneration, the reversibility of NOM e-sorption on EC PAN-EDA membranes have been further investigated in Section 3.4.

3.4. Further investigations on reversibility of EC PAN-EDA membrane

We carried out further intrinsic and e-sorption tests to investigate the lower DOC e-desorption efficiency of EC PAN-EDA at optimum cathodic potential (CP) of 2.5 V. To study the reversibility of the NOM intrinsic sorption, an EC PAN-EDA membrane was applied for intrinsic sorption (at 0 V). Following the completion of intrinsic sorption cycle ($C/C_0 = 1$), an attempt was made to e-desorb the organics adsorbed through intrinsic sorption by employing a CP of 2.5 V (Fig. 13).

The calculated DOC e-desorption efficiency of EC PAN-EDA at 2.5 V CP following intrinsic sorption was merely 23 %. In literature, full regeneration of Cr^{VI} loaded EDA functionalized chitosan by pH shift to 13 was not realized due to involvement of non-electrostatic forces (e.g., ionic interactions) [56,61]. In the current work, it was likely that adsorption of organic molecules by electrostatic forces was reversible. In contrast, adsorption of organic molecules by ionic interactions was irreversible. These results further specify that low e-desorption efficiency of EC PAN-EDA membrane material than EC PAN-NaOH might be due to marginal reversibility of intrinsic sorption by external electrical field at neutral pH conditions.

Following the e-desorption of intrinsically adsorbed NOM, e-sorption of NOM at 2.5 V AP was performed. Finally, an e-desorption cycle at 2.5 V CP was performed (Fig. 13). A higher UV_{254} removal rate was recorded during NOM e-sorption at 2.5 V AP compared to intrinsic sorption at 0 V. Likewise, UV_{254} e-desorption maxima following e-sorption was more pronounced than the e-desorption maxima following intrinsic sorption. The corresponding DOC e-sorption loading was 327 $mg{\cdot}m^{-2}$, which was higher than the solely DOC e-sorption loading (525–258 = 267 $mg{\cdot}m^{-2}$, Fig. 6). These results specified that nearly three-fourth (77 %) of intrinsic sorption might have not involved in NOM removal and only one-fourth (23 %) of intrinsic sorption might have demonstrated NOM removal during e-sorption cycle at 2.5 V AP. As a result, the DOC sorption loading at 2.5 V AP was reduced from 525 $mg{\cdot}m^{-2}$ to 327 $mg{\cdot}m^{-2}$. During e-sorption, NOM removal was mainly due to involvement of electrostatic interactions induced by external electrical field. Hence, the DOC e-desorption efficiency of the EC PAN-EDA membrane material following e-sorption at 2.5 V AP was 95 %.

Four consecutive filtration cycles (FCs) of intrinsic sorption at 0 V

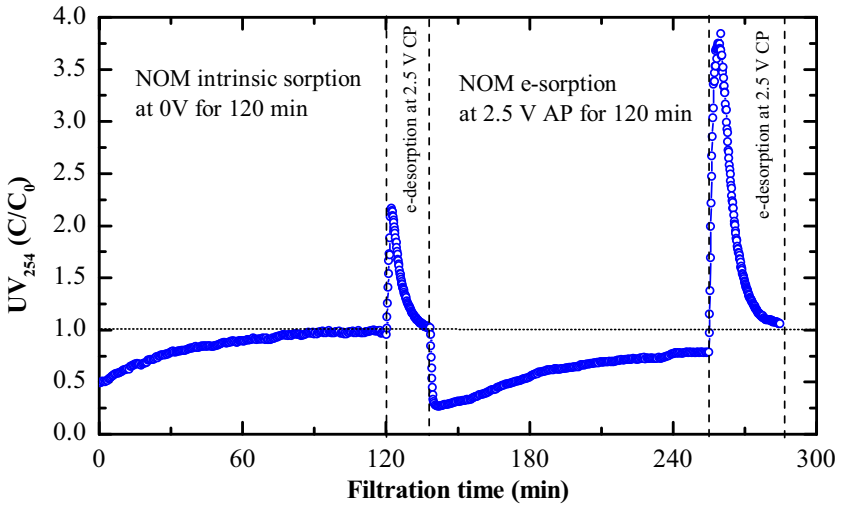

Fig. 13. UV_{254} absorbance for intrinsic sorption (at 0 V), e-sorption (at 2.5 V AP) and desorption (at 2.5 V CP) cycles for EC PAN-EDA treating feed water with SRNOM = 12 mg·L^{-1}, DOC ≈ 5 mg·L^{-1}, pH 7 and NaCl = 1 mmol·L^{-1} at permeate flux = 100 L·m^{-2}·h^{-1}.

followed by e-sorption at 2.5 V AP and e-desorption at 2.5 V CP were carried out (Fig. 14A). Each FC consisted of 120 min intrinsic sorption at 0 V, 120 min e-sorption at 2.5 V AP and 30 min e-desorption at 2.5 V CP. At the end of each FC, the electrical polarity was turned off to investigate the NOM intrinsic sorption of the PAN-EDA membrane material in cyclic operation. For comparison of normalized UV_{254} absorbance during intrinsic, e-sorption and e-desorption, all 4 FCs were plotted in parallel on same graph with same time series. Regarding NOM intrinsic sorption, UV_{254} removal decreased significantly after the first FC. This change in UV_{254} removal rate can be explained by irreversibility of intrinsic

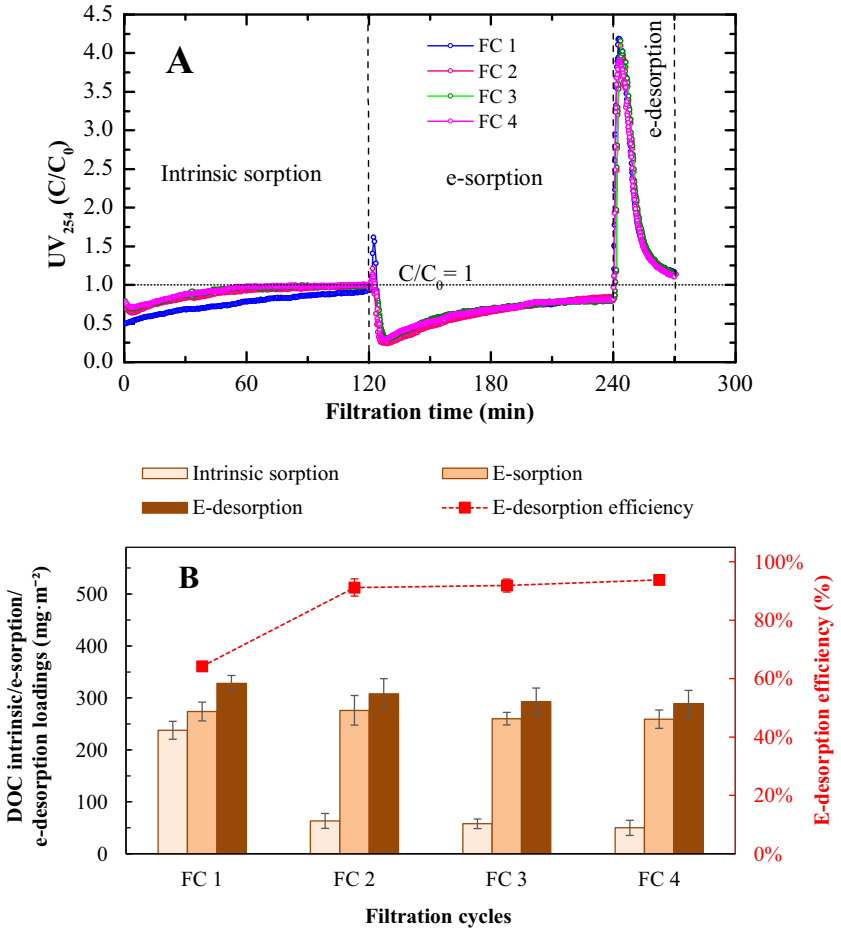

Fig. 14. (A) UV_{254} absorbance for first 4 FCs of intrinsic sorption (at 0 V), e-sorption (at 2.5 V AP) and e-desorption (at 2.5 V CP), (B) Intrinsic, e-sorption and e-desorption loadings for first 4 FCs on EC PAN-EDA. Feed water consisted of SRNOM = 12 mg·L^{-1}, DOC ≈ 5 mg·L^{-1}, pH 7 and NaCl = 1 mmol·L^{-1} and permeate flux was maintained at 100 L·m^{-2}·h^{-1}.

adsorption arising from non-electrostatic interactions (e.g., ionic interactions) in the presence of an electrical field. Regarding the e-sorption at 2.5 V AP, the UV_{254} absorbance curves of EC PAN-EDA membrane during these four FCs appeared to be the same (Fig. 14A).

The corresponding DOC intrinsic, e-sorption, and e-desorption loadings, as well as DOC

e-desorption efficiency, were calculated (Fig. 14B). The results reveal a major reduction in DOC intrinsic sorption loadings of the EC PAN-EDA membrane from FC 2 to FC 4. In FC 4, only 50 $mg{\cdot}m^{-2}$ of DOC was adsorbed. The DOC e-sorption loadings of the EC PAN-EDA for fours FCs were nearly the same (Fig. 14B). In the FC 1 to FC 4, DOC e-sorption loadings of the EC PAN-EDA membrane was decreased from 274 to 260 $mg{\cdot}m^{-2}$. The corresponding DOC e-desorption efficiency was increased from 64 % to 94 %. The increase in DOC e-desorption efficiency was resulting from decreasing DOC intrinsic adsorption loading, especially in FC 1, and almost constant DOC e-sorption loadings from FC 1 to FC 4. Moreover, the DOC e-desorption loadings are slightly higher than e-sorption loadings by 35–55 $mg{\cdot}m^{-2}$. This might be explained by additional DOC e-desorption of former intrinsically adsorbed organic molecules. Compared to EC PAN-EDA membranes, EC PAN-NaOH membranes do not exhibit intrinsic adsorption towards NOM (Fig. 5A). As a consequence, the DOC e-sorption and e-desorption loadings are almost the same (Fig. 9B SI).

The regenerated EC PAN-EDA membrane was further reused for five more consecutive e-sorption (at 2.5 V AP) and e-desorption (at 2.5 V CP) cycles (FC 5 to FC 9) to investigate its application for longer periods of electrical-field membrane filtration and the results are illustrated in Fig. 15. The NOM removal via intrinsic adsorption property of PAN-EDA membrane was not focused because NOM removal by intrinsic adsorption was practically insignificant after first 4 FCs.

In the five more consecutive e-FCs, e-sorption cycle was continued for 60 min (420 mL permeate) and e-desorption cycle was executed for 20 min. UV_{254} absorbance for these five e-sorption and e-desorption cycles (FC 5 to FC 9) was almost identical. The EC PAN-EDA membrane was able to achieve maximum UV_{254} removal of nearly 75 % at the start of e-sorption cycle and a minimum UV_{254} removal of 28 % at the end of e-sorption cycle. The e-desorption cycle was completed in 20 min and UV_{254} maxima occurred within the first 4 min. The calculated e-desorption efficiency was larger than 95 % in these five FCs. Similar results regarding UV_{254} removal was recorded using EC PAN-NaOH membrane in FC 1 – FC 4 (Fig. 9B SI). The intrinsic adsorption of the EC PAN-NaOH membrane was not targeted under cyclic operation

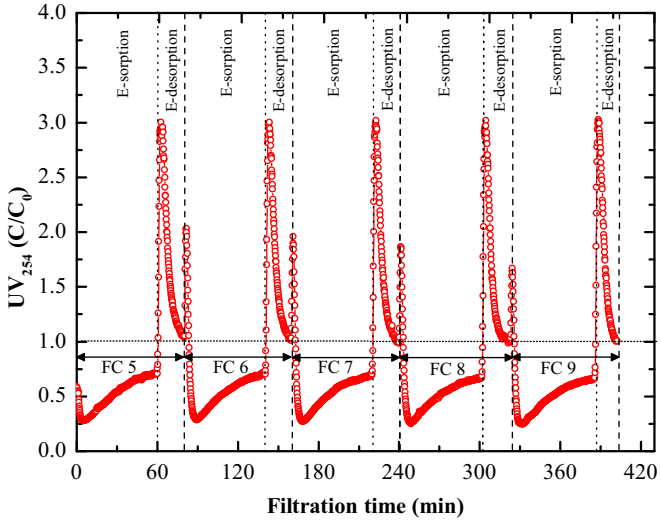

Fig. 15. NOM e-sorption (at 2.5 V AP) and desorption ((at 2.5 V CP) cycles on EC PAN-EDA membrane for five more FCs following first four FCs using same feed water at constant permeate flux of 100 $L{\cdot}m^{-2}{\cdot}h^{-1}$.

because of negligible NOM removal.

These results revealed that the presence of functional groups like amide, amine, amidine and carboxyl group in the membrane materix is indispensable not only for effective NOM e-sorption but also for e-desorption of charged substances on ECMs. In addition, these results showed that the e-sorption characteristic of the both ECMs (based on PAN-EDA and PAN-NaOH) can be successfully regenerated via electrostatic interactions of NOM with externally cathodically charged ECM and repeatedly used in removal of NOM without noticeable losses in their DOC e-sorption loadings unlike GAC adsorption [77,78]. Further, additional chemicals are not demanded for successfully regeneration of ECM unlike ion exchange resins where highly concentrated chloride brine is generated by regeneration process. Consequently, the implementation of ion exchange is limited by the burden of brine management and disposal [2,79]. SEC-OCD results have shown that the mechanism of NOM e-sorption and e-desorption on ECMs is based on electrostatic interactions and electrochemical redox reaction can be excluded. The e-sorption mechanism was found to be efficient for removal of high MW NOM and thus, NOM e-sorption would be also effective in control of DBPs precursor in raw waters comprising a large percentage of high MW NOM. In contrast, GAC adsorption is considered effective in raw waters containing a larger percentage of low MW NOM [74].

To estimate the DBPs formation potential by residual NOM, several studies have shown good relationship of UV absorbance at a specific wavelength (e.g., UV_{254}, UV_{272}, UV_{280}) with TMHs, HAAs and other DBPs [7,57]. In this work, the potential of THMs formation at UV_{280} absorbance was estimated using a linear relationship derived by Li et al., [7]. The THM potential yield of the feed water was 819 $\mu g{\cdot}L^{-1}$, which was reduced to 304 $\mu g{\cdot}L^{-1}$ after e-sorption at 2.5 V AP, indicating a decrease of 63 % in the THMs yield in the treated water.

Further, the ECMs demonstrated an excellent electrical and mechanical stability under anodic and cathodic charging conditions for 25 h. Negligible increase in electrical resistance of the ECMs was observed after using them for multiple FCs. After executing consecutive nine FCs on EC PAN-EDA membrane, Pt coating on the membrane was quite stable. The visual appearance of the EC PAN-EDA membrane was presented in Fig. 8 SI.

3.5. Impact of anodic and cathodic potential on NOM fouling of EC UF membrane

TMP was monitored at constant permeate flux of 100 $L{\cdot}m^{-2}{\cdot}h^{-1}$ to investigate NOM fouling of EC UF membrane under anodic and cathodic charging of the membranes active side. Fig. 16 illustrates variations of the TMP in NOM intrinsic sorption, e-sorption at 2.5 V AP and NOM e-desorption at 2.5 V CP on the EC PAN-EDA membrane in FC 1 - FC 4.

For intrinsic sorption, NOM fouling on ECM occurred as indicated by increase in TMP by 0.02–0.03 bar over filtration time of 120 min. The highest increase of 0.03 bar was recorded in the FC 1. When the anodic charging was applied for NOM e-sorption, measured TMP decreased by 0.03 bar (Fig. 16). This might be explained by electro-osmosis phenomenon, which occurs when the membrane matrix/pores and NOM fractions carry opposite charges. To prove the effect of electro-osmosis phenomenon on TMP at constant flux of 100 $L{\cdot}m^{-2}{\cdot}h^{-1}$, TMP was monitored for filtration of NOM free feed water (consisted of DI water with 1 $mmol{\cdot}L^{-1}$ NaCl at pH 7). By switching on anodic charging of 2.5 V to EC PAN-EDA membrane, TMP decreased by 0.02 bar (Fig. 11 SI). The contribution of electro-osmotic flow to the permeate flux was calculated to be 10.4 $L{\cdot}m^{-2}{\cdot}h^{-1}{\cdot}V^{-1}$. Regarding ECM fouling during NOM e-sorption, TMP was constant for initial 60 min of e-sorption. At the end of 120 min e-sorption, TMP increased from 0.10 bar to maximum of 0.12 bar. In general, TMP increased by 0.02 bar, indicating a comparable magnitude of NOM fouling on ECM by intrinsic sorption at 0 V, and e-sorption at 2.5 V AP.

When the electrical polarity was changed from anodic to cathodic, a sudden increase in TMP was recorded and reduced to lower increase

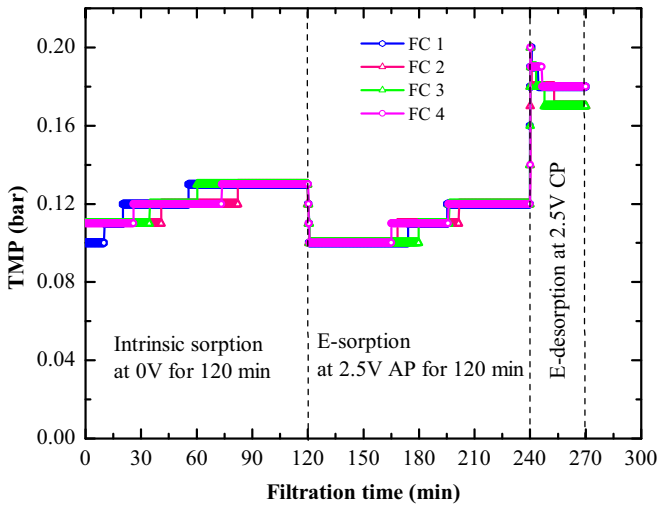

Fig. 16. Variation of TMP for NOM intrinsic sorption at 0 V, e-sorption (at 2.5 V AP) and e-desorption (at 2.5 V CP) in the treatment of feed water having SRNOM = 12 mg·L^{-1}, DOC ≈ 5 mg·L^{-1}, pH 7 and NaCl = 1 mmol·L^{-1} at constant permeate flux of 100 L·m^{-2}·h^{-1}.

within 2–3 min of NOM e-desorption from the ECM. This might be explained by the initial transport of released macromolecules through the membrane pores and matrix at CP, which will result in additional hydraulic pressure to maintain a constant permeate flux. After 2–3 min of NOM e-desorption cycle, TMP was decreased from 0.19 bar to 0.17 bar until the end of e-desorption cycle. At the end of e-desorption cycle, TMP was still larger than TMP before intrinsic and e-sorption cycles. Almost similar pattern of TMP was observed for all five FCs (FC 1 - FC 4). This might be explained by reverse direction of electro-osmotic flow because the ECM surface/pores and NOM macromolecules exhibited same charge. Analogous pattern of TMP was recorded during filtration of NOM free feed water through ECM under 2.5 V CP (Fig. 11 SI) and calculated contribution of electro-osmotic flow to permeate flux was −10.4 L·m^{-2}·h^{-1} ·V^{-1}. The electro-osmotic phenomenon have been reported earlier during NOM e-sorption at 2.5 V AP and e-desorption 2.5 V CP on Au sputtered polyamide UF membranes [32] and here contribution of electro-osmotic to permeate flux was 8 L·m^{-2}·h^{-1} ·V^{-1}. These results indicate that NOM can be efficiency removed by e-sorption on ECM and NOM fouling on ECM was negligible through this series of e-sorption cycles.

4. Conclusions

To understand the role of the functional groups on/in membrane materials in ECMs for NOM

e-sorption/e-desorption mechanisms, three membrane materials, namely, PAN, as well as PAN-NaOH, and PAN-EDA modified materials were investigated. To convert the virgin and modified PAN membranes into ECMs, an ultrathin layer of Pt was coated using magnetron sputtering on both sides of the membrane. The active side of the ECM served as working electrode and the membranes support site was the counter electrode. First, all three membrane materials were tested for their intrinsic NOM adsorption properties at neutral pH and SRNOM as a model NOM solution.

They main findings of this work are:

- At a given feed water pH, the functional groups in the membranes affects the intrinsic NOM adsorption properties of the material. PAN-EDA membrane material demonstrated NOM intrinsic adsorption capacity due to presence of amine as primary amine, whereas nitrile group, carboxyl and amide groups of PAN and PAN-NaOH membrane materials, respectively, did not show intrinsic adsorption towards NOM.
- The membrane material may exhibit NOM e-sorption characteristic, as well as e-desorption characteristic, if suitable functional groups originated from derivatives of amine along with carboxyl group are available in the matrix of membrane material.
- The DOC removal performance increases with increasing APs. At cell potential (2.5 V AP) lower than oxygen evaluation threshold of Pt, the calculated DOC e-sorption loadings of the EC PAN-EDA and PAN-NaOH membranes were 525 and 197 mg·m^{-2}. The higher performance of EC PAN-EDA membrane might be due to intrinsic adsorption property as well as due to positive intrinsic surface charge at neutral pH.
- The contact time of the NOM with membrane matrix had limited impact on the DOC e-sorption loadings at a specific external potential in electrical field-assisted membrane filtration.
- UV active organics substance such as HSs were the preferred organics for e-sorption on ECMs without leading to severe membrane fouling, while the absorbability of the remaining NOM fractions decreased with decreasing MW (i.e., building blocks > LMW acids > LWM neutrals). Hence, e-sorption process can be an efficient approach for treatment of raw waters containing large proportion of HSs. Up to 25 % of NOM could not be removed by e-sorption due to presence of uncharged NOM fractions in the feed water.
- When the applied AP was below the threshold of oxygen evolution limit, electrochemical redox reactions were absent and NOM removal was due to formation of electrostatic interactions between negatively charged organic substances and externally anodically charged ECM.
- NOM e-sorption on EC modified PAN membranes is predominantly reversible. The ECMs can be applied for a series of sorption cycles not only for removal of NOM without losing e-sorption capacity but also to concentrate charged dissolved organic substances.
- Due to the counter electrode configuration, the application of anodic charging to the ECM results in a meaningful increase in permeate flux by electro-osmotic phenomenon. The energy demand for electrical field-assisted UF filtration is quite low with approx. 20 Wh·m^{-3}.
- In future research, ultrahigh-resolution mass spectrometry (FT-ICR-MS) might be applied to determine the compositions of organic molecules in the raw and treated water samples with the highest accuracy.

CRediT authorship contribution statement

Muhammad Usman: Conceptualization, Data curation, Formal analysis, Investigation, Methodology, Project administration, Software, Validation, Visualization, Writing – original draft, Writing – review & editing. **Sarah Glass:** Conceptualization, Data curation, Formal analysis, Visualization, Writing – review & editing. **Tomi Mantel:** Conceptualization, Writing – review & editing. **Volkan Filiz:** Conceptualization, Visualization, Writing – review & editing. **Mathias Ernst:** Conceptualization, Funding acquisition, Resources, Supervision, Writing – review & editing.

Declaration of competing interest

The authors declare that they have no known competing financial interests or personal relationships that could have appeared to influence the work reported in this paper.

Data availability

Data will be made available on request.

Acknowledgement

We acknowledge the German Research Foundation (DFG) for funding this research (Project No. ER 683/1-2). We also acknowledge Dr. Martin Held, Dr. Erik Schneider and Anke Höhme (Helmholtz-Zentrum hereon GmbH) for carrying out the SEM images.

Appendix A. Supplementary data

Supplementary data to this article can be found online at https://doi.org/10.1016/j.jwpe.2023.104733.

References

[1] S. Tak, B.P. Vellanki, Natural organic matter as precursor to disinfection byproducts and its removal using conventional and advanced processes: state of the art review, J. Water Health 16 (2018) 681–703, https://doi.org/10.2166/wh.2018.032.
[2] I. Levchuk, J.J. Rueda Márquez, M. Sillanpää, Removal of natural organic matter (NOM) from water by ion exchange - a review, Chemosphere 192 (2018) 90–104, https://doi.org/10.1016/j.chemosphere.2017.10.101.
[3] G. Hasani, A. Maleki, H. Daraei, R. Ghanbari, M. Safari, G. McKay, K. Yetilmezsoy, F. Ilhan, N. Marzban, A comparative optimization and performance analysis of four different electrocoagulation-flotation processes for humic acid removal from aqueous solutions, Process. Saf. Environ. Prot. 121 (2019) 103–117, https://doi.org/10.1016/j.psep.2018.10.025.
[4] B.A.G. de Melo, F.L. Motta, M.H.A. Santana, Humic acids: structural properties and multiple functionalities for novel technological developments, Mater. Sci. Eng. C Mater. Biol. Appl. 62 (2016) 967–974, https://doi.org/10.1016/j.msec.2015.12.001.
[5] D.P. Sounthararajah, P. Loganathan, J. Kandasamy, S. Vigneswaran, Effects of humic acid and suspended solids on the removal of heavy metals from water by adsorption onto granular activated carbon, Int. J. Environ. Res. Public Health 12 (2015) 10475–10489, https://doi.org/10.3390/ijerph120910475.
[6] P.C. Singer, Humic substances as precursors for potentially harmful disinfection by-products, Water Sci. Technol. 40 (1999) 25–30, https://doi.org/10.1016/S0273-1223(99)00636-8.
[7] W.-T. Li, J. Jin, Q. Li, C.-F. Wu, H. Lu, Q. Zhou, A.-M. Li, Developing LED UV fluorescence sensors for online monitoring DOM and predicting DBPs formation potential during water treatment, Water Res. 93 (2016) 1–9, https://doi.org/10.1016/j.watres.2016.01.005.
[8] X.-F. Li, W.A. Mitch, Drinking water disinfection byproducts (DBPs) and human health effects: multidisciplinary challenges and opportunities, Environ. Sci. Technol. 52 (2018) 1681–1689, https://doi.org/10.1021/acs.est.7b05440.
[9] C.D. Peters, T. Rantissi, V. Gitis, N.P. Hankins, Retention of natural organic matter by ultrafiltration and the mitigation of membrane fouling through pre-treatment, membrane enhancement, and cleaning - a review, J. Water Process. Eng. 44 (2021) 102374, https://doi.org/10.1016/j.jwpe.2021.102374.
[10] Sillanpää, M.; Metsämuuronen, S.; Mänttäri, M. Membranes. Natural Organic Matter in Water; Elsevier, 2015; pp. 113–157, (ISBN 9780128015032.).
[11] Z. Su, T. Liu, X. Li, N. Graham, W. Yu, Beneficial impacts of natural biopolymers during surface water purification by membrane nanofiltration, Water Res. 201 (2021) 117330, https://doi.org/10.1016/j.watres.2021.117330.
[12] A.K. Camper, Involvement of humic substances in regrowth, Int. J. Food Microbiol. 92 (2004) 355–364, https://doi.org/10.1016/j.ijfoodmicro.2003.08.009.
[13] P.-L. Rantanen, M.M. Keinänen-Toivola, M. Ahonen, A. González-Martínez, I. Mellin, R. Vahala, Decreased natural organic matter in water distribution decreases nitrite formation in non-disinfected conditions, via enhanced nitrite oxidation, Water Res. X 9 (2020) 100069, https://doi.org/10.1016/j.wroa.2020.100069.
[14] X. Zhu, D. Jassby, Electroactive membranes for water treatment: enhanced treatment functionalities, energy considerations, and future challenges, Acc. Chem. Res. 52 (2019) 1177–1186, https://doi.org/10.1021/acs.accounts.8b00558.
[15] J. Benecke, Gypsum Scaling during Reverse Osmosis Desalination – Characterization and Effects of Natural Organic Matter, PhD thesis;, Technische Universität Hamburg, Hamburg, Germany, 2018.
[16] A. Lidén, K.M. Persson, Comparison between ultrafiltration and nanofiltration hollow-fiber membranes for removal of natural organic matter–a pilot study, J. Water Supply Res Technol. jws2015065 (2015), https://doi.org/10.2166/aqua.2015.065.
[17] H. Guo, X. Li, W. Yang, Z. Yao, Y. Mei, L.E. Peng, Z. Yang, S. Shao, C.Y. Tang, Nanofiltration for drinking water treatment: a review, Front. Chem. Sci. Eng. 16 (2022) 681–698, https://doi.org/10.1007/s11705-021-2103-5.
[18] H. Rosentreter, M. Walther, A. Lerch, Partial desalination of saline groundwater: comparison of nanofiltration, reverse osmosis and membrane capacitive deionisation, Membranes (Basel) 11 (2021), https://doi.org/10.3390/membranes11020126.
[19] H. Chang, Y. Zhu, H. Yu, F. Qu, Z. Zhou, X. Li, Y. Yang, X. Tang, H. Liang, Long-term operation of ultrafiltration membrane in full-scale drinking water treatment plants in China: characteristics of membrane performance, Desalination 543 (2022) 116122, https://doi.org/10.1016/j.desal.2022.116122.
[20] C. Cordier, C. Stavrakakis, B. Morga, L. Degrémont, A. Voulgaris, A. Bacchi, P. Sauvade, F. Coelho, P. Moulin, Removal of pathogens by ultrafiltration from sea water, Environ. Int. 142 (2020) 105809, https://doi.org/10.1016/j.envint.2020.105809.
[21] N. Jacquet, S. Wurtzer, G. Darracq, Y. Wyart, L. Moulin, P. Moulin, Effect of concentration on virus removal for ultrafiltration membrane in drinking water production, J. Membr. Sci. 634 (2021) 119417, https://doi.org/10.1016/j.memsci.2021.119417.
[22] X. Guo, Z. Zhang, L. Fang, L. Su, Study on ultrafiltration for surface water by a polyvinylchloride hollow fiber membrane, Desalination 238 (2009) 183–191, https://doi.org/10.1016/j.desal.2007.11.064.
[23] H. Yu, H. Chang, X. Li, Z. Zhou, W. Song, H. Ji, H. Liang, Long-term fouling evolution of polyvinyl chloride ultrafiltration membranes in a hybrid short-length sedimentation/ ultrafiltration process for drinking water production, J. Membr. Sci. 630 (2021) 119320, https://doi.org/10.1016/j.memsci.2021.119320.
[24] J. Lowe, M. Hossain, Application of ultrafiltration membranes for removal of humic acid from drinking water, Desalination 218 (2008) 343–354, https://doi.org/10.1016/j.desal.2007.02.030.
[25] C.-F. Lin, Y.-J. Huang, O.J. Hao, Ultrafiltration processes for removing humic substances: effect of molecular weight fractions and PAC treatment, Water Res. 33 (1999) 1252–1264, https://doi.org/10.1016/S0043-1354(98)00322-4.
[26] K. Konieczny, D. Sąkol, J. Płonka, M. Rajca, M. Bodzek, Coagulation—ultrafiltration system for river water treatment, Desalination 240 (2009) 151–159, https://doi.org/10.1016/j.desal.2007.11.072.
[27] X. Cui, K.-H. Choo, Natural organic matter removal and fouling control in low-pressure membrane filtration for water treatment, Environ. Eng. Res. 19 (2014) 1–8, https://doi.org/10.4491/eer.2014.19.1.001.
[28] X. Cheng, P. Li, W. Zhou, D. Wu, C. Luo, W. Liu, Z. Ren, H. Liang, Effect of peroxymonosulfate oxidation activated by powdered activated carbon for mitigating ultrafiltration membrane fouling caused by different natural organic matter fractions, Chemosphere 221 (2019) 812–823, https://doi.org/10.1016/j.chemosphere.2019.01.081.
[29] M. Wang, Q. Cen, R. Zeng, Y. Huang, Y. Liu, S. Xia, Performance of a hybrid process integrating PAC adsorption with ceramic membrane ultrafiltration for drinking water treatment, J. Environ. Chem. Eng. 10 (2022) 108427, https://doi.org/10.1016/j.jece.2022.108427.
[30] Z. Zhang, J. Wu, L. Shao, L. Wang, X. Yang, B. Zhao, J. Li, C. Ma, X. Chu, P. Zhang, Comparison between integrated MIEX/UF and PAC/UF in long-term irreversible membrane fouling reduction: effectiveness and mechanism analysis, Process Saf. Environ. Prot. 168 (2022) 1179–1187, https://doi.org/10.1016/j.psep.2022.10.068.
[31] J. Li, Z. Zhang, T. Li, B. Zhao, Y. Liu, Y. Liu, L. Wang, D.D. Dionysiou, Efficient synergism of K2FeO4 preoxidation/ MIEX adsorption in ultrafiltration membrane fouling control and mechanisms, J. Membr. Sci. 648 (2022) 120331, https://doi.org/10.1016/j.memsci.2022.120331.
[32] T. Mantel, E. Jacki, M. Ernst, Electrosorptive removal of organic water constituents by positively charged electrically conductive UF membranes, Water Res. 201 (2021) 117318, https://doi.org/10.1016/j.watres.2021.117318.
[33] Z. Zhang, G. Huang, Y. Li, X. Chen, Y. Yao, S. Ren, M. Li, Y. Wu, C. An, Electrically conductive inorganic membranes: a review on principles, characteristics and applications, Chem. Eng. J. 427 (2022) 131987, https://doi.org/10.1016/j.cej.2021.131987.
[34] M. Sun, X. Wang, L.R. Winter, Y. Zhao, W. Ma, T. Hedtke, J.-H. Kim, M. Elimelech, Electrified membranes for water treatment applications, ACS EST Eng. 1 (2021) 725–752, https://doi.org/10.1021/acsestengg.1c00015.
[35] T. Mantel, P. Benne, M. Ernst, Electrically conducting duplex-coated gold-PES-UF membrane for capacitive organic fouling mitigation and rejection enhancement, J. Membr. Sci. 620 (2021) 118831, https://doi.org/10.1016/j.memsci.2020.118831.
[36] W. Duan, G. Chen, C. Chen, R. Sanghvi, A. Iddya, S. Walker, H. Liu, A. Ronen, D. Jassby, Electrochemical removal of hexavalent chromium using electrically conducting carbon nanotube/polymer composite ultrafiltration membranes, J. Membr. Sci. 531 (2017) 160–171, https://doi.org/10.1016/j.memsci.2017.02.050.
[37] A. Ronen, S.L. Walker, D. Jassby, Electroconductive and electroresponsive membranes for water treatment, Rev. Chem. Eng. 32 (2016), https://doi.org/10.1515/revce-2015-0060.
[38] X. Fan, H. Zhao, X. Quan, Y. Liu, S. Chen, Nanocarbon-based membrane filtration integrated with electric field driving for effective membrane fouling mitigation, Water Res. 88 (2016) 285–292, https://doi.org/10.1016/j.watres.2015.10.043.
[39] S. Ma, F. Yang, X. Chen, C.M. Khor, B. Jung, A. Iddya, G. Sant, D. Jassby, Removal of As(III) by electrically conducting ultrafiltration membranes, Water Res. 204 (2021) 117592, https://doi.org/10.1016/j.watres.2021.117592.
[40] P. Formoso, E. Pantuso, G. Filpo, de; Nicoletta, F.P., Electro-conductive membranes for permeation enhancement and fouling mitigation: a short review, Membranes (Basel) 7 (2017), https://doi.org/10.3390/membranes7030039.
[41] P. Sivasubramanian, M. Kumar, V.S. Kirankumar, M.S. Samuel, C.-D. Dong, J.-H. Chang, Capacitive deionization and electrosorption techniques with different electrodes for wastewater treatment applications, Desalination 559 (2023) 116652, https://doi.org/10.1016/j.desal.2023.116652.
[42] J. Chen, K. Zuo, Y. Li, X. Huang, J. Hu, Y. Yang, W. Wang, L. Chen, A. Jain, R. Verduzco, et al., Eggshell membrane derived nitrogen rich porous carbon for

selective electrosorption of nitrate from water, Water Res. 216 (2022) 118351, https://doi.org/10.1016/j.watres.2022.118351.
[43] C. Wang, R. Li, Y. Xu, Z. Ma, Y. Qiu, C. Wang, L.-F. Ren, J. Shao, Effective electrosorption and recovery of phosphorus by capacitive deionization with a covalent organic framework-membrane coating electrode, Desalination 570 (2024) 117088, https://doi.org/10.1016/j.desal.2023.117088.
[44] Y. Zhao, N. Mamrol, W.A. Tarpeh, X. Yang, C. Gao, B. van der Bruggen, Advanced ion transfer materials in electro-driven membrane processes for sustainable ion-resource extraction and recovery, Prog. Mater. Sci. 128 (2022) 100958, https://doi.org/10.1016/j.pmatsci.2022.100958.
[45] J.D. Ritchie, E. Perdue, Proton-binding study of standard and reference fulvic acids, humic acids, and natural organic matter, Geochim. Cosmochim. Acta 67 (2003) 85–96, https://doi.org/10.1016/S0016-7037(02)01044-X.
[46] S. Glass, T. Mantel, M. Appold, S. Sen, M. Usman, M. Ernst, V. Filiz, Amine-terminated PAN membranes as anion-adsorber materials, Chem. Ing. Tech. 93 (2021) 1396–1400, https://doi.org/10.1002/cite.202100037.
[47] M.H. El-Newehy, A. Alamri, S.S. Al-Deyab, Optimization of amine-terminated polyacrylonitrile synthesis and characterization, Arab. J. Chem. 7 (2014) 235–241, https://doi.org/10.1016/j.arabjc.2012.04.041.
[48] A.A. Kishore Chand, B. Bajer, E.S. Schneider, T. Mantel, M. Ernst, V. Filiz, S. Glass, Modification of polyacrylonitrile ultrafiltration membranes to enhance the adsorption of cations and anions, Membranes (Basel) 12 (2022), https://doi.org/10.3390/membranes12060580.
[49] J. Park, S.H. Park, S.-H. Jeong, J.-Y. Lee, J.Y. Song, Corrosion behavior of silver-coated conductive yarn, Front. Chem. 11 (2023) 1090648, https://doi.org/10.3389/fchem.2023.1090648.
[50] T. Mantel, S. Glass, M. Usman, A. Lyberis, V. Filiz, M. Ernst, Adsorptive dead-end filtration for removal of Cr(VI) using novel amine modified polyacrylonitrile ultrafiltration membranes, Environ. Sci.: Water Res. Technol. 8 (2022) 2981–2993, https://doi.org/10.1039/D2EW00570K.
[51] T. Luxbacher, The Zeta Potential for Solid Surface Analysis: A Practical Guide to Streaming Potential Measurement, 1st edition, Graz, Austria, Anton Paar GmbH, 2014.
[52] M. Schulz, A. Soltani, X. Zheng, M. Ernst, Effect of inorganic colloidal water constituents on combined low-pressure membrane fouling with natural organic matter (NOM), J. Membr. Sci. 507 (2016) 154–164, https://doi.org/10.1016/j.memsci.2016.02.008.
[53] Huber, S.A.; Balz, A.; Abert, M.; Pronk, W. Characterisation of aquatic humic and non-humic matter with size-exclusion chromatography–organic carbon detection–organic nitrogen detection (LC-OCD-OND). Water Res. 2011, 45, 879–885, doi: https://doi.org/10.1016/j.watres.2010.09.023.
[54] N. Li, Y. Fu, Q. Lu, C. Xiao, Microstructure and performance of a porous polymer membrane with a copper nano-layer using vapor-induced phase separation combined with magnetron sputtering, Polymers (Basel) 9 (2017), https://doi.org/10.3390/polym9100524.
[55] S. Krainer, U. Hirn, Contact angle measurement on porous substrates: effect of liquid absorption and drop size, Colloids Surf. A Physicochem. Eng. Asp. 619 (2021) 126503, https://doi.org/10.1016/j.colsurfa.2021.126503.
[56] X. Hu, J. Wang, Y. Liu, X. Li, G. Zeng, Z. Bao, X. Zeng, A. Chen, F. Long, Adsorption of chromium (VI) by ethylenediamine-modified cross-linked magnetic chitosan resin: isotherms, kinetics and thermodynamics, J. Hazard. Mater. 185 (2011) 306–314, https://doi.org/10.1016/j.jhazmat.2010.09.034.
[57] Saha, P.; Nam, C.; Hickner, M.A.; Zenyuk, I.V. Electrokinetic streaming-current methods to probe the electrode–electrolyte interface under applied potentials. J. Phys. Chem. C 2019, 123, 19493–19505, doi:https://doi.org/10.1021/acs.jpcc.9b03430.
[58] E. Drzymała, G. Gruzeł, A. Pajor-Świerzy, J. Depciuch, R. Socha, A. Kowal, P. Warszyński, M. Parlinska-Wojtan, Design and assembly of ternary Pt/Re/SnO2 NPs by controlling the zeta potential of individual Pt, Re, and SnO2 NPs, J. Nanopart. Res. 20 (2018) 144, https://doi.org/10.1007/s11051-018-4244-0.
[59] G. Marzun, C. Streich, S. Jendrzej, S. Barcikowski, P. Wagener, Adsorption of colloidal platinum nanoparticles to supports: charge transfer and effects of electrostatic and steric interactions, Langmuir 30 (2014) 11928–11936, https://doi.org/10.1021/la502588g.
[60] X.-Y. Huang, J.-P. Bin, H.-T. Bu, G.-B. Jiang, M.-H. Zeng, Removal of anionic dye eosin Y from aqueous solution using ethylenediamine modified chitosan, Carbohydr. Polym. 84 (2011) 1350–1356, https://doi.org/10.1016/j.carbpol.2011.01.033.
[61] S.T. Ong, C.K. Lee, Z. Zainal, Removal of basic and reactive dyes using ethylenediamine modified rice hull, Bioresour. Technol. 98 (2007) 2792–2799, https://doi.org/10.1016/j.biortech.2006.05.011.
[62] Y. Tan, W. Huang, Q. Lei, S. Huang, K. Yang, X. Chen, D. Li, Insight into the adsorption of magnetic microspheres with large mesopores: tailoring mesoporous structure and ethylenediamine functionalization for ultrahigh Congo red removal, Sep. Purif. Technol. 311 (2023) 123265, https://doi.org/10.1016/j.seppur.2023.123265.
[63] M. Gussoni, M. Rui, G. Zerbi, Electronic and relaxation contribution to linear molecular polarizability. An analysis of the experimental values, J. Mol. Struct. 447 (1998) 163–215, https://doi.org/10.1016/S0022-2860(97)00292-5.
[64] T. Mahfoud, G. Molnár, S. Bonhommeau, S. Cobo, L. Salmon, P. Demont, H. Tokoro, S.-I. Ohkoshi, K. Boukheddaden, A. Bousseksou, Electric-field-induced charge-transfer phase transition: a promising approach toward electrically switchable devices, J. Am. Chem. Soc. 131 (2009) 15049–15054, https://doi.org/10.1021/ja9055855.
[65] X. Liu, J. Wu, J. Wang, Electro-enhanced removal of cobalt ions from aqueous solution by capacitive deionization, Sci. Total Environ. 697 (2019) 134144, https://doi.org/10.1016/j.scitotenv.2019.134144.
[66] X. Liu, J. Wang, Electro-adsorption characteristics and mechanism of Sr2+ ions by capacitive deionization and CFD analysis study, Prog. Nucl. Energy 133 (2021) 103628, https://doi.org/10.1016/j.pnucene.2020.103628.
[67] A.V. Dudchenko, J. Rolf, K. Russell, W. Duan, D. Jassby, Organic fouling inhibition on electrically conducting carbon nanotube–polyvinyl alcohol composite ultrafiltration membranes, J. Membr. Sci. 468 (2014) 1–10, https://doi.org/10.1016/j.memsci.2014.05.041.
[68] M. Shuang, L. Zhou, Y. Liu, H. Yu, X. Ao, J. Ouyang, Z. Liu, H. Shehzad, A. A. Adesina, Electrodeposition nanofabrication of graphene oxide/polypyrrole electrodes with high hybrid specific capacitance for enhancing U(VI) electrosorption, J. Environ. Chem. Eng. 111498 (2023), https://doi.org/10.1016/j.jece.2023.111498.
[69] I. Caltran, S. Heijman, H.L. Shorney-Darby, L.C. Rietveld, Impact of removal of natural organic matter from surface water by ion exchange: a case study of pilots in Belgium, United Kingdom and the Netherlands, Sep. Purif. Technol. 247 (2020) 116974, https://doi.org/10.1016/j.seppur.2020.116974.
[70] O. Kaarela, M. Koppanen, T. Kesti, R. Kettunen, M. Palmroth, J. Rintala, Natural organic matter removal in a full-scale drinking water treatment plant using ClO2 oxidation: performance of two virgin granular activated carbons, J. Water Process. Eng. 41 (2021) 102001, https://doi.org/10.1016/j.jwpe.2021.102001.
[71] L. Tian, P. Zhou, Z. Su, T. Liu, N. Graham, T. Bond, W. Yu, Insights into the properties of surface waters and their associated nanofiltration membrane fouling: the importance of biopolymers and high molecular weight humics, Chem. Eng. J. 451 (2023) 138682, https://doi.org/10.1016/j.cej.2022.138682.
[72] B. Bolto, D. Dixon, R. Eldridge, Ion exchange for the removal of natural organic matter, React. Funct. Polym. 60 (2004) 171–182, https://doi.org/10.1016/J.REACTFUNCTPOLYM.2004.02.021.
[73] B. Bolto, D. Dixon, R. Eldridge, S. King, K. Linge, Removal of natural organic matter by ion exchange, Water Res. 36 (2002) 5057–5065, https://doi.org/10.1016/S0043-1354(02)00231-2.
[74] S. Velten, D.R.U. Knappe, J. Traber, H.-P. Kaiser, U. von Gunten, M. Boller, S. Meylan, Characterization of natural organic matter adsorption in granular activated carbon adsorbers, Water Res. 45 (2011) 3951–3959, https://doi.org/10.1016/j.watres.2011.04.047.
[75] J. Kim, B. Kang, DBPs removal in GAC filter-adsorber, Water Res. 42 (2008) 145–152, https://doi.org/10.1016/j.watres.2007.07.040.
[76] C.J. Hwang, S. Krasner, M. Sclimenti, Polar NOM: Characterization, DBPs, Treatment, American Water Works Association, 2001.
[77] R.M. Narbaitz, J. McEwen, Electrochemical regeneration of field spent GAC from two water treatment plants, Water Res. 46 (2012) 4852–4860, https://doi.org/10.1016/j.watres.2012.05.046.
[78] C.-A. Chiu, K. Hristovski, S. Huling, P. Westerhoff, In-situ regeneration of saturated granular activated carbon by an iron oxide nanocatalyst, Water Res. 47 (2013) 1596–1603, https://doi.org/10.1016/j.watres.2012.12.021.
[79] M. Sillanpää, Natural Organic Matter in Water: Characterization and Treatment Methods, Butterworth-Heinemann, 2014.